

Precise deletion, replacement and inversion of large DNA fragments in plants using dual prime editing

Received: 22 April 2024

Accepted: 11 December 2024

Published online: 13 January 2025

 Check for updates

Yidi Zhao^{1,5}, Zhengwei Huang^{1,5}, Ximeng Zhou^{1,5}, Wan Teng^{① 2,5}, Zehua Liu¹, Wenping Wang¹, Shengjia Tang^{2,3}, Ying Liu⁴, Jing Liu¹, Wenxi Wang^{① 1}, Lingling Chai¹, Na Zhang⁴, Weilong Guo^{① 1}, Jie Liu^{① 1}, Zhongfu Ni^{① 1}, Qixin Sun^{① 1}, Yanpeng Wang^{① 2,3}✉ & Yuan Zong^{① 1}✉

Precise manipulation of genome structural variations holds great potential for plant trait improvement and biological research. Here we present a genome-editing approach, dual prime editing (DualPE), that efficiently facilitates precise deletion, replacement and inversion of large DNA fragments in plants. In our experiments, DualPE enabled the production of specific genomic deletions ranging from ~500 bp to 2 Mb in wheat protoplasts and plants. DualPE was effective in directly replacing wheat genomic fragments of up to 258 kb with desired sequences in the absence of donor DNA. Additionally, DualPE allowed precise DNA inversions of up to 205.4 kb in wheat plants with efficiencies of up to 51.5%. DualPE also successfully edited large DNA fragments in the dicots *Nicotiana benthamiana* and tomato, with editing efficiencies of up to 72.7%. DualPE thus provides a precise and efficient approach for large DNA sequence and chromosomal engineering, expanding the availability of precision genome-editing tools for crop improvement.

Improving agronomic traits relies on the exploitation and manipulation of plant genetic variation, ranging from single nucleotide polymorphisms to large structural variants^{1,2}. In particular, structural variants, such as large deletions, replacements and inversions, represent a major source of genetic diversity and play critical roles in genome evolution and the genetic control of agronomic traits in plants^{3,4}. While the efficiency and precision of current CRISPR–Cas-based genome-editing technologies, such as nucleases, base editors and prime editors, have been substantially improved for plant genome editing, the technologies largely remain limited to making small changes, such as the introduction of base substitutions and small insertions or deletions (indels)^{5,6}. The manipulation of larger DNA fragments, such as large deletions,

replacements and inversions in the tens of kilobases, remains a great challenge in plant genomes^{7,8}.

CRISPR–Cas nucleases, such as Cas9, induce double-strand breaks (DSBs) in targeted DNA, leading to the introduction of small indels through the non-homologous end-joining repair pathway^{9,10}. The paired single guide RNAs (sgRNAs) with Cas9 nuclease can induce genome structural variants, including large deletions^{11–15}, inversions^{16–21} and even inter-chromosomal translocations²² in plants. However, this approach primarily produces indels, with more complex structural edits being much less frequent and often mixed with varied outcomes^{5,23}. Alternatively, large DNA fragments can be edited through homology-directed repair when a donor DNA template is provided^{24,25}.

¹Frontiers Science Center for Molecular Design Breeding (MOE), Key Laboratory of Crop Heterosis and Utilization (MOE) and Beijing Key Laboratory of Crop Genetic Improvement, China Agricultural University, Beijing, China. ²Center for Genome Editing, Institute of Genetics and Developmental Biology, Chinese Academy of Sciences, Beijing, China. ³College of Advanced Agricultural Sciences, University of Chinese Academy of Sciences, Beijing, China. ⁴College of Horticulture, China Agricultural University, Beijing, China. ⁵These authors contributed equally: Yidi Zhao, Zhengwei Huang, Ximeng Zhou, Wan Teng. ✉e-mail: yanpengwang@genetics.ac.cn; zongyuan@cau.edu.cn

However, homology-directed repair shows low efficiency, and the delivery of donor DNA templates into plant cells remains challenging⁷. This approach also introduces many undesired outcomes, such as random indels or more complex chromosomal rearrangements due to the presence of DSBs^{23–25}.

Prime editing (PE) is a precision genome-editing technique, based on a fusion between the Cas9 nickase (H840A) and a reverse transcriptase (RT), that uses a modified PE guideRNA (pegRNA) comprising an RT template (RTT) and a primer-binding site (PBS), enabling the genetic writing of small edits²⁶. The RT uses the nicked genomic DNA strand as a primer for the synthesis of an edited DNA flap templated by an extension on the pegRNA. Subsequent DNA repair incorporates the edited 3' flap, permanently installing the programmed edit²⁶. PE can precisely install any base substitution as well as small indels (generally <30 bp) in plant genomes, but it is currently limited to short modifications^{5,27,28}. Although recent advances in combining PE with a site-specific recombinase system (Cre-loxP) have enabled the insertion of DNA fragments up to 11.1 kilobases (kb) into rice and maize cells²⁹, there is still a need to improve the efficiency of this approach and to extend its application for engineering other types of genome structural variations.

Recently, advanced PE-based methods, such as PRIME-Del³⁰, PEDAR³¹, twinPE³², GRAND³³, PETI³⁴ and AE³⁵, have successfully facilitated the manipulation of large DNA fragments in mammalian cells. Instead of using a single pegRNA as done in the canonical PE approach, these methods use two pegRNAs targeting opposite strands. Specifically, PRIME-Del, twinPE and GRAND incorporate a Cas9 nickase-RT fusion (nCas9-RT) along with two protospacer adjacent motif (PAM)-in pegRNAs for deletions, replacements or insertions of up to the kilobase level^{30,32,33}. PEDAR and PETI, in contrast, use a wild-type (WT) Cas9 nuclease-RT fusion (Cas9-RT) with two pegRNAs to achieve deletions of 1–10 kb with a short insertion, as well as inversions, or translocations of DNA fragments up to megabase (Mb) sizes^{31,34}. However, PEDAR and PETI methods exhibit lower accuracy due to the use of Cas9-RT, which introduces DSBs^{31,34}. Additionally, the AE system employs nCas9-RT and a pair of PAM-out pegRNAs, enabling programmable DNA duplication with precision at the chromosomal scale³⁵. These studies indicate that the combination of nCas9-RT with two pegRNAs holds substantial potential for precise large-scale DNA editing. Despite the rapid expansion of the genome-editing toolbox in mammalian cells, there is still a lack of genome-editing tools that can efficiently and precisely engineer large genome structural variations in plants.

Here we present an efficient and precise method called dual prime editing (DualPE), comprising a plant-optimized prime editor (ePPEplus)³⁶ and dual engineered pegRNAs (epegRNAs). DualPE outperformed other genome-editing methods in facilitating scarless deletions, replacements and inversions of large chromosomal segments up to 2 Mb in wheat, *Nicotiana benthamiana* and tomato without requiring DSBs or a repair template. We also developed the web server DualPE-Finder to facilitate dual-pegRNA design for large DNA fragment editing. DualPE is thus a new approach for efficiently and precisely engineering the structure of plant genomes and holds great promise for crop trait improvement.

Results

Overview of DualPE

To facilitate genome structural variation engineering in plants, we used an optimized prime editor, ePPEplus, which contains a V223A mutation in the RT and R221K and N394K mutations in nCas9 (H840A)³⁶, with dual epegRNAs (hereafter referred to as pegL and pegR) to target complementary DNA strands with a PAM-in orientation. The ePPEplus-epegRNA complex recognizes the target sites adjacent to the large DNA fragment being edited and nicks the PAM-containing DNA strands. The 3' ends of the nicking sites hybridize to the corresponding PBS of pegRNA and then reverse transcribe RTTs, generating two 3' DNA flaps

at the respective target sites. Theoretically, as depicted in Fig. 1, it is possible to achieve large DNA deletions, replacements or inversions through manipulating these 3' DNA flaps (Fig. 1). There are three possible scenarios. First, if each 3' flap sequence is complementary to the region targeted by the other pegRNA, the two 3' flaps will anneal to form double-stranded DNA, resulting in the excision of the original DNA strands (5' flaps). The subsequent DNA repair process leads to the precise deletion of DNA fragments between the two pegRNAs (Fig. 1, left). Second, in cases where the two 3' flaps generated by the RTT are partially complementary to each other and also contain a desired insertion sequence, two 3' flaps annealing, followed by DNA synthesis and excision of the 5' flaps, results in a deletion and simultaneous insertion of the desired sequence between the two pegRNAs (Fig. 1, middle). Third, when each 3' flap sequence is complementary to the inverted region targeted by the other pegRNA, each 3' flap will anneal to its corresponding sequence (Fig. 1, right). This annealing will serve as a primer to initiate DNA synthesis in the opposite orientation. Subsequently, the 5' flaps will be excised, followed by ligation and DNA repair, which may result in an inversion. These three scenarios represent the genome-editing approach that we term dual prime editing or DualPE.

Efficiency and precision of DualPE-mediated DNA deletions

To assess the efficiency and precision of DualPE for large DNA deletions in plant cells, we compared DualPE with two other editing strategies: WT-DualPE (restoring the mutated Ala840 of nCas9 to the original His840 in DualPE) combined with a pair of epegRNAs, and Cas9 combined with a pair of esgRNAs (flip and extension (F + E) sgRNAs) (Supplementary Figs. 1 and 2). We randomly selected and designed seven targeted deletions with lengths ranging from about 500 bp to over 365 kb (that is, 507 bp, 1.5 kb, 2.3 kb, 4.8 kb, 79.3 kb, 258.0 kb and 365.9 kb) in wheat genomic loci (Fig. 2a). For DualPE and WT-DualPE, the 30-bp RTTs in the pairs of epegRNAs (pegL and pegR) are complementary to the DNA sequence in each targeted deletion site, while the two esgRNAs (sgL and sgR) for Cas9 are designed to recognize the same sites as the epegRNAs (Supplementary Fig. 3 and Supplementary Table 1). For each targeted deletion, we transfected wheat protoplasts with pegL and pegR along with DualPE or WT-DualPE, or sgL and sgR with Cas9, to test the efficiency of these editors (Supplementary Fig. 1). To avoid overestimating the efficiency due to the shorter, edited templates being favoured by both PCR and Illumina-based sequencing, typically for edited fragments >200 bp, we used digital PCR (dPCR) with fluorescence readout of TaqMan probes to evaluate the deletion efficiencies (Supplementary Fig. 4 and Supplementary Table 2).

Digital PCR analysis showed that DualPE can induce deletion events with frequencies ranging from 0.1% to 30.9% (Fig. 2a and Extended Data Fig. 1). In three out of seven cases (for the 507-bp, 1.5-kb and 2.3-kb deletions), DualPE was more efficient at inducing the deletion than WT-DualPE and Cas9. In another three of seven cases (for the 4.8-kb, 258.0-kb and 365.9-kb deletions), DualPE, WT-DualPE and Cas9 exhibited comparable efficiency. For the 79.3-kb deletion, DualPE efficiency was 0.1%, which was lower than that of WT-DualPE and Cas9 (Fig. 2a and Extended Data Fig. 1). Nonetheless, DualPE generally resulted in higher deletion efficiencies across tested sites than Cas9 and WT-DualPE, corresponding to an average 3.3-fold (up to 11.3-fold) and 1.2-fold (up to 2.6-fold) increased efficiency over Cas9 and WT-DualPE, respectively (Fig. 2b). Notably, DualPE efficiently deleted fragments up to several hundred kilobases, with efficiencies of 4.8% for the 258.0-kb deletion and 5.8% for the 365.9-kb deletion, whose sizes are larger than the largest previously reported deletion in mammalian cells of 10 kb^{30–32}.

To assess editing accuracy, we purified the PCR amplicons spanning the deletion site for high-throughput amplicon sequencing (Supplementary Figs. 5 and 6). DualPE had a significantly higher level of accurate editing at each target site, with an average of 95.3% accuracy across all deletion events (ranging from 83.9% to 99.1%), thus higher than the averages of 31.5% (ranging from 6.4% to 58.8%) for WT-DualPE

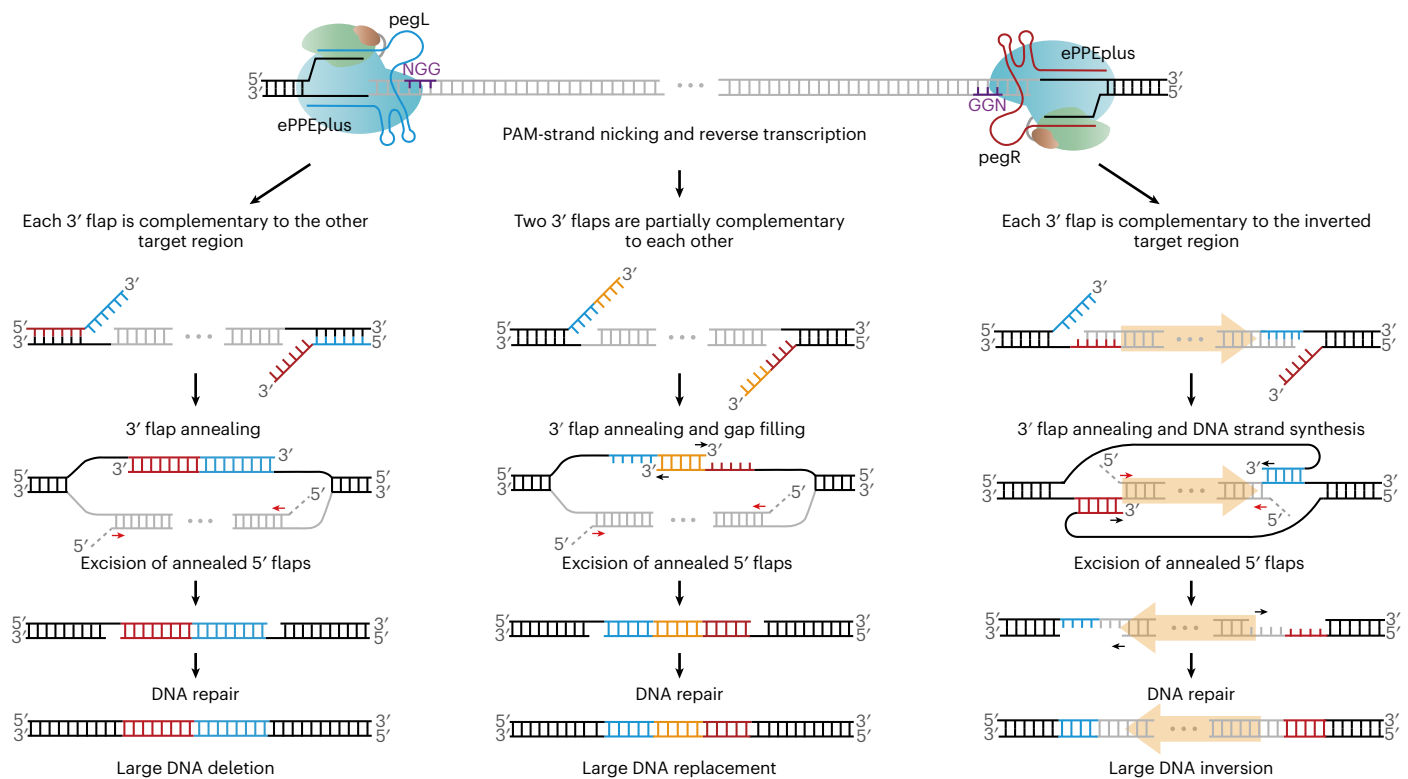


Fig. 1 | Overview of DualPE-mediated large DNA deletions, replacements and inversions. Two pegRNAs (pegL and pegR) define the sites to be nicked at each end of the intended edit. For deletions, each 3' flap is complementary to the other target region. For replacements, the two 3' DNA flaps are partially

complementary to each other and harbour the edits. The inserted sequences are shown in blue, yellow and red. Homologous overlap between two 3' DNA flaps is shown in yellow. For inversions, each 3' DNA flap is complementary to the other target region at the inversion junction.

and 21.3% (ranging from 0.0% to 56.4%) for Cas9 (Fig. 2c,d and Supplementary Fig. 6). Sanger sequencing of the amplicons confirmed this result (Extended Data Fig. 2). We noticed that although WT-DualPE and Cas9 achieved a higher efficiency for deleting the 79.3-kb region than DualPE (Fig. 2a), they also produced a much higher rate of imprecise deletions (93.6% for WT-DualPE and 96.0% for Cas9, compared with 0.9% for DualPE; Fig. 2c and Extended Data Fig. 2). Taken together, these results indicate that DualPE outperforms the WT-DualPE and Cas9 editing strategies in programming accurate large-fragment deletions in wheat cells.

DualPE creates precise large chromosomal deletions in wheat

To explore the robustness of DualPE in producing large DNA deletions, we tested its performance in transgenic wheat plants in deleting large chromosomal segments. We employed *Agrobacterium tumefaciens*-mediated transformation to introduce a binary expression vector containing a dual-epgRNA array designed for a deletion of approximately 365.9 kb (Fragment 7) in wheat plants (Fig. 2e and Extended Data Fig. 3a). To assess the deletion frequency, we extracted genomic DNA from the leaves of transgenic wheat plants for PCR amplification with two pairs of primers: one pair to amplify the WT sequence and the other pair to produce a PCR amplicon specific to the deletion. From an examination of 19 individual regenerated plants, we identified two plants harbouring large deletions (Fig. 2f). Both mutant plants harboured the desired precise 365.9-kb deletion, with one plant (T_0 -8) being homozygous and the other (T_0 -13) being heterozygous for the deletion (Fig. 2f-h). We allowed the T_0 -8 and T_0 -13 plants to self-pollinate and analysed their T_1 progenies. The examined T_1 plants from T_0 -8 were all homozygous for the 365.9-kb deletion, while the deletion segregated with a typical Mendelian pattern in the T_1 progeny from T_0 -13 (Extended Data Fig. 3b-d).

These results suggest that DualPE can create heritable large DNA deletions in wheat plants.

Furthermore, to evaluate the length limits of DualPE in stable transgenic plants, we targeted one additional site to introduce a 2-Mb deletion (Fragment 8). We identified one plant harbouring the precise 2-Mb deletion among 13 regenerated T_0 wheat plants using the indicated primers (Fig. 2h,i and Supplementary Fig. 7). Overall, DualPE enables the generation of precise chromosomal segment deletions in wheat, greatly broadening the applicability of PE for targeting large genome sequences in plants.

Simultaneous large deletion and insertion using DualPE

Next, we tested whether DualPE would concurrently introduce a defined insertion at the site of deletion in wheat cells. As depicted in Fig. 1, DualPE-mediated replacement needs paired pegRNAs with partial complementary RTTs that encode the sequences for the desired insertion (Fig. 1, middle). Because it bypasses the need for any homologous DNA sequence in the targeted genome, this approach offers more flexibility in choosing template sequences for replacement. We randomly targeted three loci in wheat protoplasts to replace 60 bp of endogenous sequence with a 38-bp *attP* substrate sequence, replace 41 bp with a 50-bp *attP* substrate sequence or replace 96 bp with a 90-bp sequence encoding a 3xHA tag (Fig. 3a and Supplementary Table 3). We compared DualPE with WT-DualPE for these replacement events (Supplementary Fig. 8). For each replacement, we designed dual epgRNAs with a roughly 30-bp overlap of the RTT between the pegL and pegR (Supplementary Fig. 9a). When dual epgRNAs were transfected into wheat protoplasts along with DualPE or WT-DualPE, we obtained a significantly higher rate of replacement events with DualPE (average 33.8%) than with WT-DualPE (average 11.8%) at the three sites tested, reaching up to 43.0% (Fig. 3a). The results demonstrate that DualPE

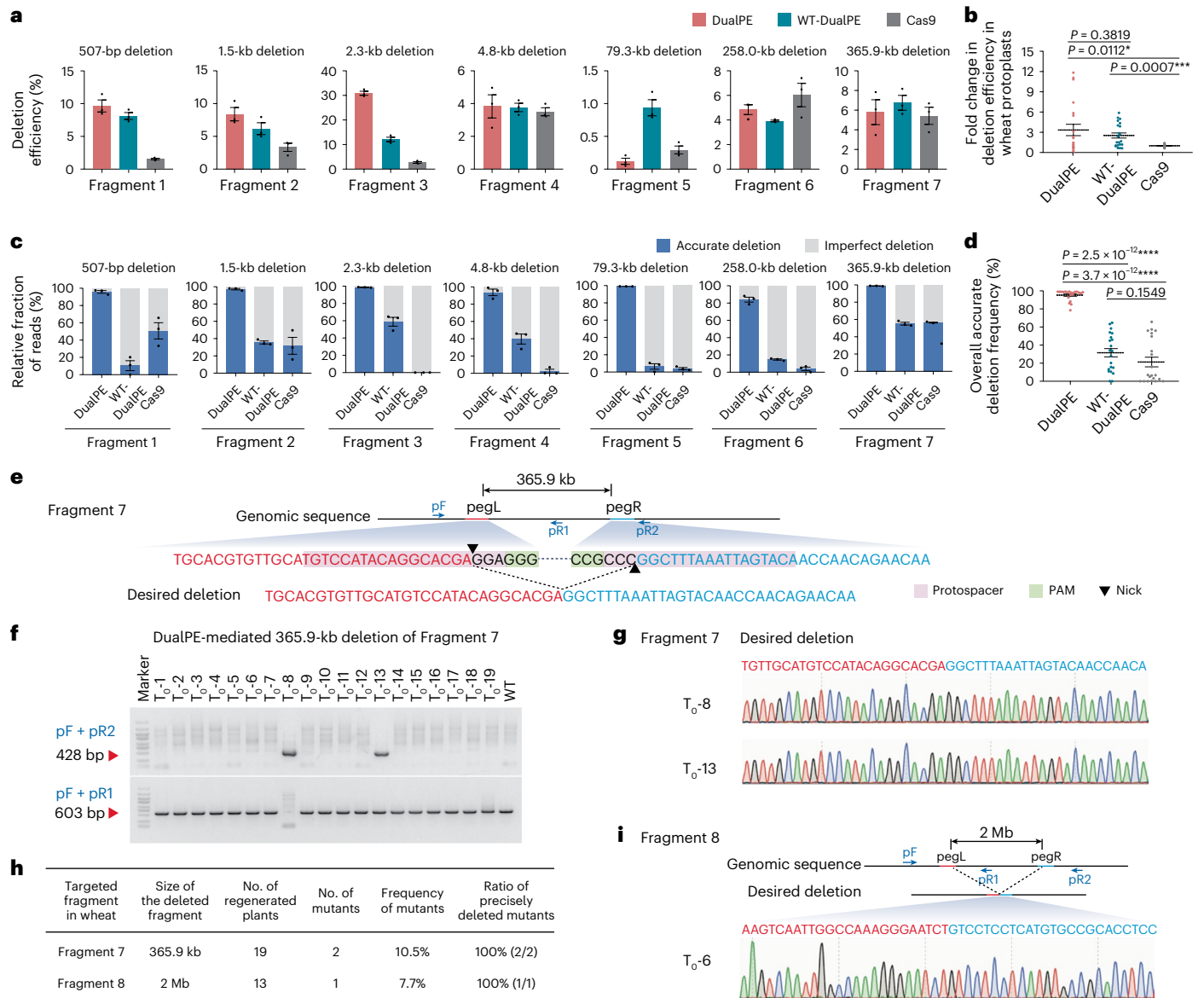


Fig. 2 | Precise large DNA deletions in wheat using the DualPE system.

a, Percentage of deletion efficiency at seven endogenous loci induced by DualPE, WT-DualPE and Cas9, as measured by dPCR. **b**, Summary of the fold change in deletion efficiency for DualPE and WT-DualPE compared with Cas9. The editing frequencies using Cas9 for each target were set to 1, and the frequencies using DualPE and WT-DualPE for each target were adjusted accordingly. **c**, Fraction of reads with an accurate or imperfect deletion for all deletion events shown in **a**. The fraction shown in the plot was calculated as the number of reads with the indicated editing/total deletion events. **d**, Overall fraction of reads with an accurate deletion across all targeted loci. The values and error bars in **a–d** represent means and standard errors of the mean of three independent

biological replicates. The *P* values were obtained from two-tailed Student's *t*-tests in **b** and **d**: **P* < 0.05; ****P* < 0.001; *****P* < 0.0001. **e**, Overview of Fragment 7 and Sanger sequencing primers for evaluating the 365.9-kb deletion at Fragment 7. pF, pR1 and pR2 are the primers used for PCR and Sanger sequencing. **f**, Representative agarose gel electrophoresis of PCR products for genotyping of the deletion. The 428-bp band is the desired size for the deletion, while the 603-bp band is the expected size for the WT sequence. **g**, Sanger sequencing chromatograms of the precise 365.9-kb deletion in the T₀-8 and T₀-13 plants. **h**, Summary of DualPE-mediated deletion frequency for the 365.9-kb and 2-Mb deletions in wheat plants. **i**, Overview of Fragment 8 and Sanger sequencing chromatograms for evaluating the 2-Mb deletion at Fragment 8.

can replace stretches of nearly 100 bp in the genome of wheat cells with one pair of epegRNAs.

We investigated the limits of DualPE with respect to deletion size and concurrent insertion. Accordingly, we designed dual epegRNAs at randomly selected sites to introduce three additional deletions of 713 bp, 4.8 kb and 258.0 kb, with a 34-bp *lox76* insertion. Digital PCR analysis revealed that DualPE achieves insertions after such larger deletions, with frequencies of 23.8%, 7.3% and 0.4% at the three sites, respectively. In contrast, WT-DualPE exhibited significantly lower insertion frequencies of 2.3%, 0.3% and 0.1% at the same sites (Fig. 3b and Supplementary Fig. 9b–e). This observation is consistent with our

results for shorter deletions and insertions (Fig. 3a). In total, DualPE generated 8.7-fold higher editing efficiencies than WT-DualPE across the six tested loci for simultaneous deletion and insertion (Fig. 3c). As anticipated, the results showed that DualPE achieved highly accurate replacement editing in all six cases tested, with an average efficiency of 93.5% (up to 98.9%), far exceeding that of WT-DualPE (with an average efficiency of 32.1%, up to 55.2%), with which by-products of direct deletions and imperfect replacements were more common (Fig. 3d,e, Extended Data Fig. 4 and Supplementary Fig. 10). Overall, these data demonstrate the robustness, flexibility and precision of DualPE in generating >250-kb deletions and up to 90-bp insertions in plant cells.

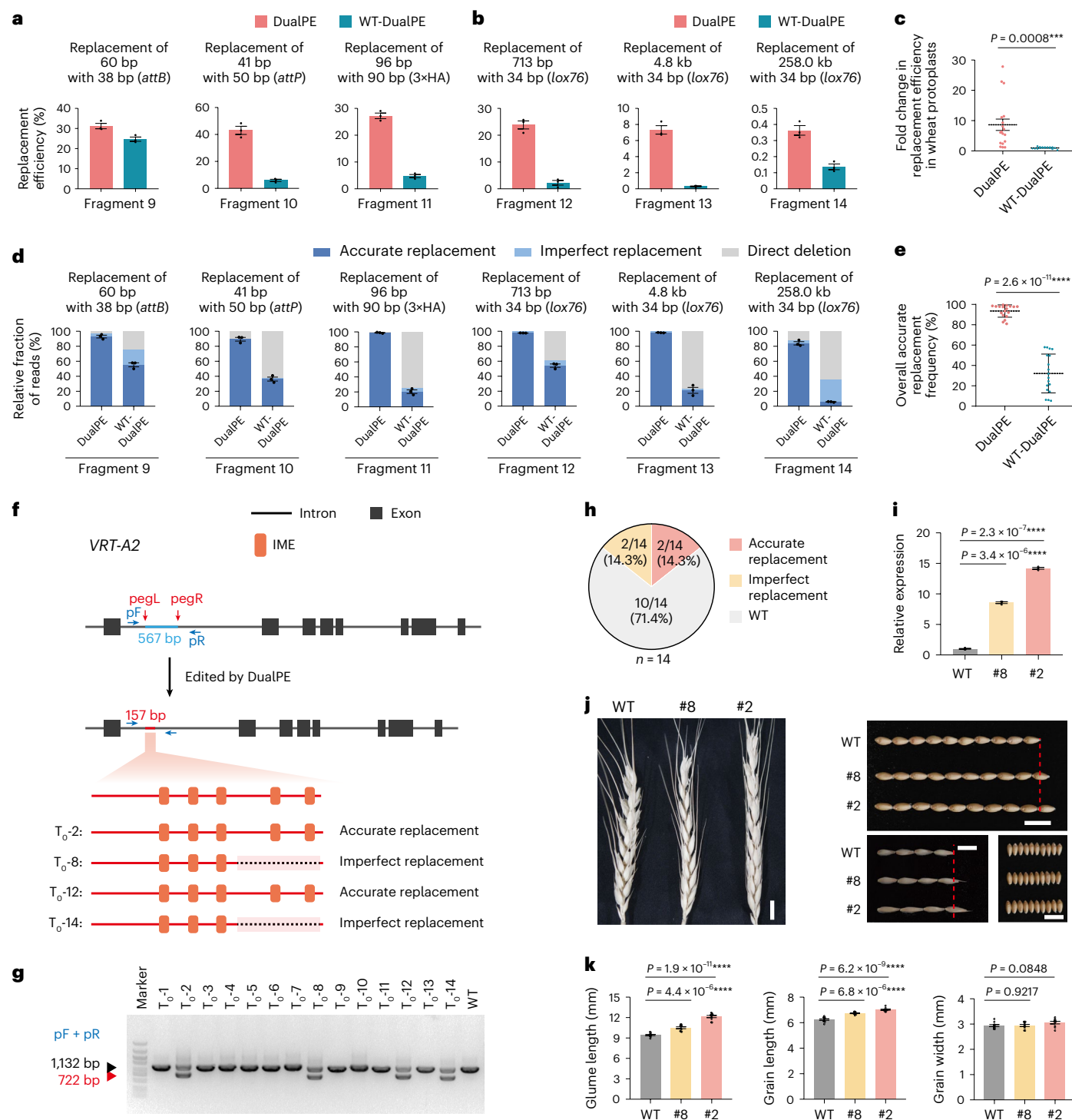


Fig. 3 | DualPE-mediated sequence replacement in wheat. **a**, Replacement rates at three endogenous loci induced by DualPE and WT-DualPE, as measured by high-throughput amplicon sequencing. **b**, Percentage efficiency of replacements at three endogenous loci induced by DualPE and WT-DualPE, as measured by dPCR. **c**, Summary of the fold change in replacement efficiency for DualPE compared with WT-DualPE. The editing frequencies using WT-DualPE for each target were set to 1, and the frequencies using DualPE for each target were adjusted accordingly. **d**, Fraction of reads with a precise replacement, an imperfect replacement or a direct deletion. The editing rate represents the number of reads with the indicated editing/total deletion events. **e**, Overall fraction of reads with precise replacement across all targeted loci. **f**, Replacement strategy at the *VRT-A2* locus and evaluation of the results. The 567-bp fragment

(blue) was replaced with a 157-bp sequence (red) containing five IME elements. **g**, Gel electrophoresis of PCR products for genotyping of the replacement. The 722-bp band is the desired product with replacement, while the 1,132-bp band is the WT sequence. **h**, Summary of DualPE-mediated replacement of the 567-bp sequence with the 157-bp sequence in wheat plants. **i**, qRT-PCR analysis of relative *VRT-A2* expression levels in the WT and mutants. **j**, Representative spike and glume phenotypes, and grain traits of the WT and mutants. Scale bars, 1 cm. **k**, Glume length, grain length and grain width of mutants and the WT. The data are calculated from the values collected from ten independent plants. The values and error bars in **a–e** and **i** represent means and standard errors of the mean of three independent biological replicates. The *P* values were obtained from two-tailed Student's *t*-tests in **c**, **e**, **i** and **k**: ****P* < 0.001; *****P* < 0.0001.

DualPE enables gene activation by replacements in wheat

One potential application for DualPE-mediated editing would be to replace regulatory elements and modify gene expression patterns. To test this idea, we turned to a naturally occurring sequence rearrangement reported as a key ON/OFF molecular switch for *VEGETATIVE TO REPRODUCTIVE TRANSITION-A2* (*VRT-A2*) expression and control of glume length^{37–40}. Specifically, the replacement of a 560-bp sequence by a 157-bp sequence containing five copies of intron-mediated enhancement (IME) elements in the first intron of *VRT-A2* drives the ectopic expression of *VRT-A2* in floral organs, resulting in the long-glume phenotype of the tetraploid wheat species *Triticum polonicum* and the hexaploid wheat *T. petropavlovskyi*^{37–40}. We hypothesized that DualPE might allow the introduction of this sequence replacement at the *VRT-A2* locus in the hexaploid spring wheat variety ‘Fielder’ to regulate *VRT-A2* expression and increase glume length. We thus designed pegL and pegR with a roughly 90-bp RTT covering the insertion fragment (157 bp) and sharing 30 bp of homozygous sequence to replace the original 567-bp sequence (the 560-bp sequence plus a 7-bp flanking sequence for PAM design; Fig. 3f and Extended Data Fig. 5a). We introduced the binary expression vector into immature ‘Fielder’ embryos, obtaining 14 T₀ transgenic wheat seedlings. We amplified the target genomic site and identified four plants with mutations (Fig. 3f–h). Of these four plants, two (T₀-2 and T₀-12) harboured the precisely intended 567-bp deletion and the 157-bp insertion containing all five IME motifs; we confirmed this result by Sanger sequencing (Extended Data Fig. 5b). The two remaining plants (T₀-8 and T₀-14) harboured a 109-bp replacement containing three of the five IME motifs in place of the 567-bp fragment (Fig. 3f–h and Extended Data Fig. 5b), possibly due to the presence of repetitive IMEs in the complementary RTT.

To examine the effect of the sequence replacement by the IME motifs, we measured *VRT-A2* transcript levels by quantitative reverse transcription PCR (qRT-PCR) assay in homozygous T₁ progeny from the T₀-2 and T₀-8 plants (Extended Data Fig. 5c). Indeed, the insertion of IME elements resulted in higher *VRT-A2* expression, with expression levels being positively associated with the number of IME elements present (Fig. 3i). In addition, both lines developed elongated glumes and much longer grains than those of the WT, while grain width was not altered (Fig. 3j,k). These phenotypes are consistent with recent transgenic studies with overexpression of a genomic fragment containing the desired variation of *VRT-A2* (refs. 37,38,40). Overall, our data demonstrate the potential of DualPE for creating precise and larger replacements into the genome related to major agronomic traits for crop improvement, even for sequences containing repetitive elements.

DualPE produces accurate large inversions in wheat

Inversions can influence plant adaptation potential and gene function by affecting gene expression and preventing recombination⁴. To investigate whether DualPE can facilitate large DNA inversions in plants, we designed a pair of epegRNAs containing an RTT that transcribes a 3' flap (-30-bp) complementary to the other target region at the inversion junction. As shown in Fig. 1, each 3' flap anneals with its complementary DNA sequences. This annealing prime DNA synthesis uses one strand of the sequence between the two nicks as a template and thus inverts the sequence of interest (Fig. 1, right). We randomly chose five genomic loci for editing, with the goal of producing inversions of about 713 bp, 1.5 kb, 2.6 kb, 74.4 kb and 252.6 kb. We also designed WT-DualPE and Cas9 as controls (Supplementary Figs. 11 and 12a). After wheat protoplasts were transformed, dPCR analysis showed that DualPE generated inversions with frequencies of 8.4%, 0.4%, 1.5%, 0.2% and 0.2% for the 713-bp, 1.5-kb, 2.6-kb, 74.4-kb and 252.6-kb inversions, respectively. The frequencies using WT-DualPE were 1.8%, 0.7%, 0.4%, 0.8% and 0.2%, respectively, and the frequencies using Cas9 were 2.2%, 0.6%, 0.7%, 0.5% and 1.4%, respectively (Fig. 4a and Supplementary Fig. 12b–g). More importantly, we conducted targeted deep sequencing and Sanger

sequencing using inversion-specific primer pairs. The results revealed that DualPE induced a significantly higher fraction of precise inversions, with averages of 98.8% at the left junction (Junction-L) and 95.2% at the right junction (Junction-R). In contrast, WT-DualPE showed averages of 51.3% at Junction-L and 38.6% at Junction-R, while Cas9 exhibited averages of 38.1% at Junction-L and 33.6% at Junction-R (Fig. 4b,c and Extended Data Fig. 6). Therefore, DualPE could successfully achieve precise DNA fragment inversions in wheat protoplasts.

Next, to test the potential of DualPE for large inversion editing in stable transgenic wheat plants, we chose three wheat sites for inversions of 7.4, 19.2 and 82.8 kb. In the regenerated plants, we identified inversion events using PCR with four pairs of primers: two pairs to amplify the WT sequence and the other two pairs to produce a PCR amplicon specific to the inversion at Junction-L and Junction-R. We obtained 85, 19 and 23 mutant plants for the 7.4-kb, 19.2-kb and 82.8-kb inversions, respectively, with inversion mutation efficiencies of 51.5%, 31.7% and 21.9%, respectively (Fig. 4d). Seamless inversions were observed in 68.2% of the mutant plants with the 7.4-kb inversion, 57.9% of those with the 19.2-kb inversion and 100% of those with the 82.8-kb inversion, at both Junction-L and Junction-R (Fig. 4d and Extended Data Fig. 7). Moreover, homozygous mutants were identified with efficiencies of 11.8% for the 7.4-kb inversion and 5.3% for the 19.2-kb inversion among mutants (Extended Data Fig. 7a–d). Indels were observed at inverted Junction-L of the 7.4-kb inversion mutants, primarily due to the presence of micro-homologous sequences at Junction-L (Extended Data Fig. 7b). In addition, a single nucleotide polymorphism was detected at the inverted Junction-R of the 7.4-kb and at the inverted Junction-R of the 19.2-kb inversion mutants (Extended Data Fig. 7b,d). This occurrence was largely due to by-products derived from the pegRNA scaffold, which could be eliminated using the termination rule for the design of pegRNAs⁴¹. These results show that DualPE is a straightforward and efficient method to induce inversions of nearly hundreds of kilobases in scale without altering the sequences at the junction sites in wheat plants.

One potential application of DualPE-mediated inversions is swapping promoters between two nearby genes with diverging promoters to regulate gene expression. To test whether DualPE could achieve promoter swapping, we targeted the *Suppressor of gamma response 1* (*SOG1*) gene and the *Gibberellic acid-stimulated regulator 7* (*GASR7*) gene on the short arm of chromosome 7B, which have different expression patterns⁴². We designed pegL, between the promoter and coding region of *GASR7*, and pegR, between the promoter and coding region of *SOG1*, to swap the *GASR7* and *SOG1* promoters. The designed inversion was about 205.4 kb (Fig. 4e). Using inversion-specific primers on both ends of the intended inversions, we identified 32 wheat plants with the precise 205.4-kb inversion among 116 regenerated plants (Fig. 4d–g). To assess whether the gene expression levels changed after promoter swapping, we used qRT-PCR to measure the expression levels of the two genes. The transcript accumulation of *GASR7* was significantly decreased to 3.7–4.9-fold, while that of *SOG1* was enhanced to approximately 2.0-fold when compared with their levels in the WT (Fig. 4h). Collectively, these data demonstrate that DualPE is effective for generating large inversions for promoter swapping in wheat, which should benefit crop improvement through the editing of large and/or complex functional gene variants. Importantly, this demonstrates that a prime editor can produce over 200-kb inversions in plants, leaving no scar at the junctions of inversion fragments.

DualPE facilitates large DNA fragment editing in dicots

To test whether DualPE could enable large DNA editing in dicot plant species, we tested it in *N. benthamiana* leaves via a transient *Agrobacterium*-mediated infiltration system with a vector. The vector carries a 2×35S promoter to drive the expression of ePPEplus and the *Cestrum Yellow Leaf Curling Virus* (CmYLCV) promoter to drive the expression of two epegRNAs using the Csy-type ribonuclease 4 (Csy4)

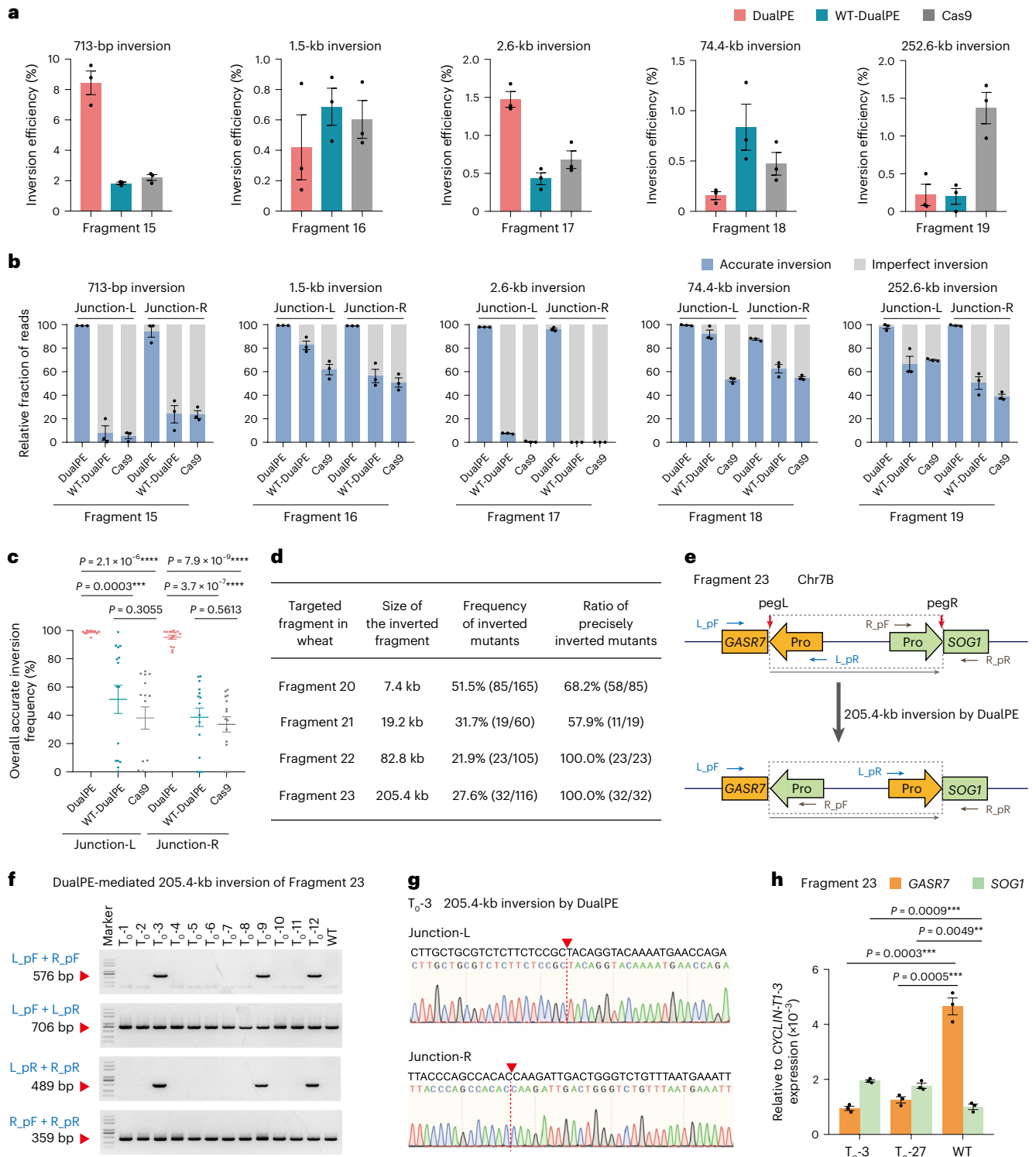


Fig. 4 | Use of DualPE to generate large DNA inversions in wheat. a, Frequency of inversion for the 713-bp, 1.5-kb, 2.6-kb, 74.4-kb and 252.6-kb inversions induced by DualPE, WT-DualPE and Cas9, as measured by dPCR. **b**, Fraction of precise inversion events and inversion with unwanted indels at Junction-L and Junction-R, as determined by targeted deep sequencing of amplicons generated using inversion-specific primers. The editing rate represents the number of reads with the indicated editing/total inversion events. **c**, Overall fraction of reads with precise inversion across all targeted loci at Junction-L and Junction-R. **d**, Summary of DualPE-mediated inversion frequencies for the 7.4-kb, 19.2-kb, 82.8-kb and 205.4-kb inversions in wheat plants. **e**, Promoter swap between *GASR7* and *SOG1* on chromosome 7B by designed inversions. The primer pairs L_pF + L_pR and R_pF + R_pR were used to evaluate the WT sequence. The primer

pairs L_pF + R_pF and L_pR + R_pR were used to identify events with inversions; only events with an inversion can produce PCR products with these primer pairs. **f**, Representative agarose gel of PCR products for genotyping the inversion. The 576-bp and 489-bp bands are the desired bands for Junction-L and Junction-R of the inversion, respectively, while the 706-bp and 359-bp bands are the expected sizes for the WT sequence. **g**, Sanger sequencing chromatograms of the precise 205.4-kb promoter swap inversion between *GASR7* and *SOG1* mediated by DualPE in the T₀-3 wheat plant. **h**, qRT-PCR analysis of relative *GASR7* and *SOG1* expression levels in WT and mutant plants (T₀-3 and T₀-27). The values and error bars in **a–c** and **h** represent means and standard errors of the mean of three independent biological replicates. The *P* values were obtained from two-tailed Student's *t*-tests in **c** and **h**: ***P* < 0.01; ****P* < 0.001; *****P* < 0.0001.

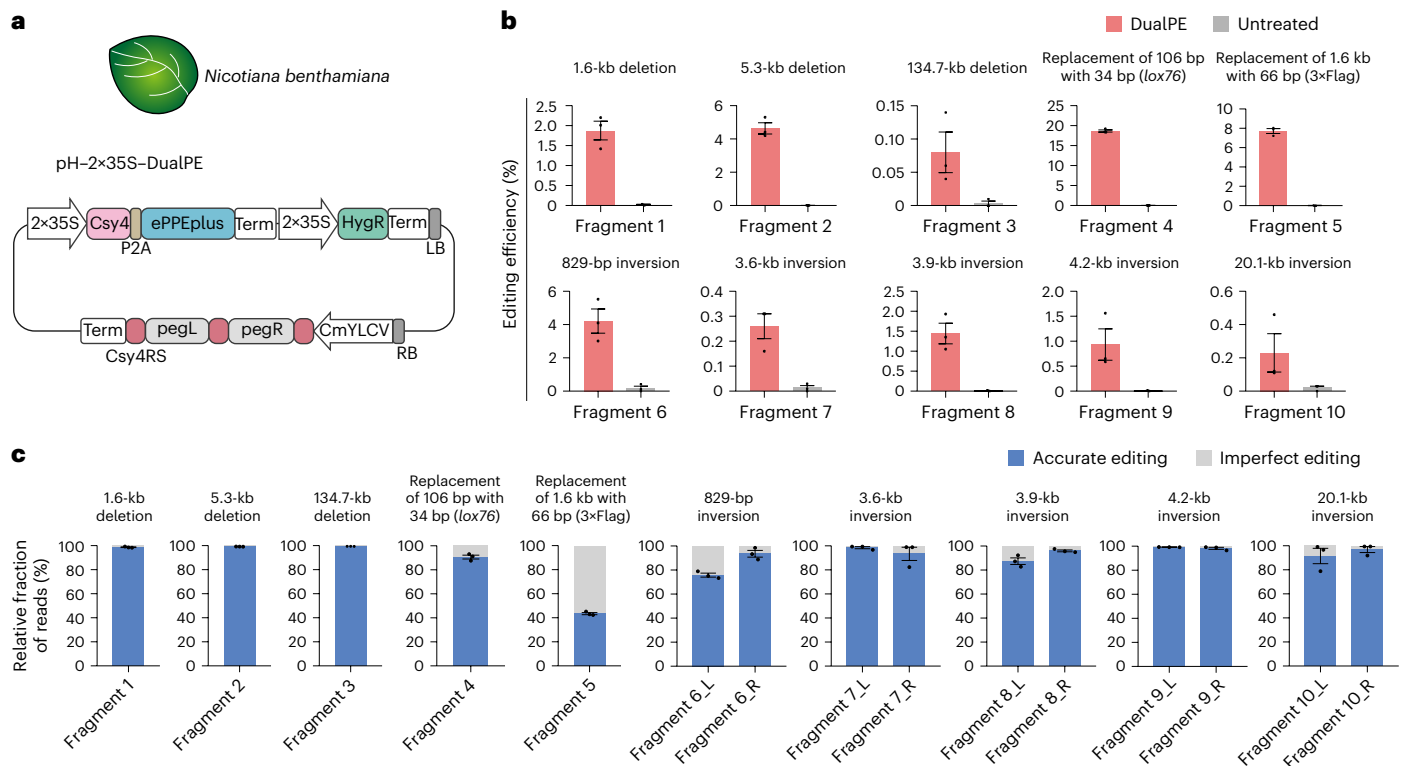


Fig. 5 | DualPE enables large DNA editing in *N. benthamiana*. **a**, The pH-2x35S-DualPE construct used for *N. benthamiana* DNA editing. **b**, Frequency for the 1.6-kb deletion, 5.3-kb deletion, 134.7-kb deletion, 106-bp deletion with a 34-bp replacement, 1.6-kb deletion with a 66-bp replacement, 829-bp inversion, 3.6-kb inversion, 3.9-kb inversion, 4.2-kb inversion and 20.1-kb inversion induced by DualPE in *N. benthamiana* cells, as measured by dPCR. **c**, Fraction of reads with

precise editing and imperfect editing for deletions, replacements and inversions. The editing rate represents the number of reads with the indicated editing/total editing events. L and R represent Junction-L and Junction-R, respectively. The values and error bars in **b** and **c** represent means and standard errors of the mean of three independent biological replicates.

strategy (Fig. 5a). We selected ten endogenous *N. benthamiana* loci covering deletion, replacement and inversion editing types for testing—namely, a 1.6-kb deletion, a 5.3-kb deletion, a 134.7-kb deletion, a 106-bp deletion with a 34-bp insertion, a 1.6-kb deletion with a 66-bp insertion, a 829-bp inversion, a 3.6-kb inversion, a 3.9-kb inversion, a 4.2-kb inversion and a 20.1-kb inversion. Digital PCR analysis showed that DualPE resulted in editing at all tested sites, with efficiencies of up to 4.6% for deletions, 18.7% for replacements and 4.2% for inversions, even for edits larger than 10 kb, with an activity of approximately 0.1% for the 134.7-kb deletion and 0.2% for the 20.1-kb inversion (Fig. 5b). We found that DualPE harbours high accuracy (Fig. 5c and Extended Data Fig. 8a–j), except for Fragment 5, whose accuracy (43.4%) may be influenced by the repetitive sequence of the 3xFlag intended for insertion (Extended Data Fig. 8e).

We also evaluated DualPE performance in tomato. CmYLCV was used to drive the expression of two epegRNAs using the Csy4 processing system, and the *EF1 α* promoter was used to drive the expression of ePPEplus (Fig. 6a), which was previously proved to have high activity in base editing⁴³. In the protoplast assay, DualPE displayed editing activities of about 0.1% for a 725-bp deletion and 1.3% for a 1.1-kb inversion with high precision (Fig. 6b,c and Extended Data Fig. 8k,l). DualPE also induced precise larger DNA edits, as indicated by a 5.3-kb deletion and a 9.6-kb inversion in protoplasts (Fig. 6d,e). We next evaluated the capacity of DualPE to edit large DNA fragments in stable transgenic tomato plants. Our results revealed remarkable efficiencies for DualPE: 70.0% for a 725-bp deletion, 43.5% for a 725-bp inversion, 72.7% for a 1.1-kb deletion with a 38-bp insertion and 45.0% for a 9.6-kb deletion with a 34-bp insertion. Furthermore, we achieved homozygous mutations with efficiencies as high as 27.3% (Fig. 6f–h and Extended Data

Fig. 9). These results show that DualPE can efficiently induce editing of large DNA fragments of up to hundreds of kilobases for deletion, replacement and inversion in *N. benthamiana* and tomato, offering new opportunities for applying prime editors in dicot plants. Collectively, our results indicate that DualPE could be a robust large DNA editing tool for monocot and dicot plant species.

DualPE-Finder web server for editing large DNA fragments

To facilitate chromosome editing via DualPE, we developed a Python-based web server, DualPE-Finder (available at http://wheat.cau.edu.cn/DualPE_Finder/), that automates the design procedure of dual-pegRNA (Fig. 7a). For a given DualPE experiment, such as deletion, replacement or inversion, DualPE-Finder requires a single input consisting of the reference and intended edited information (Extended Data Fig. 10 and see details in Methods). First, the web server searches for protospacers and PAM sequences flanking the desired editing site. If a suitable PAM is unavailable, a feature titled ‘Accept the range for protospacers search’ will be offered. With this option, the web server will carry out searches within the ranges specified by the user, expanding around both the starting and ending positions of the intended edit fragment. Second, the web server facilitates dual-pegRNA design according to user-specified parameters, including PBS length, recommended melting temperature (T_m) of the PBS sequence, RTT length or homology overlap length between two RTTs, and the option to exclude the first C in the RTT. Upon finalizing the target sequence search, PBS and RTT designs, the web server proceeds to design the corresponding primers, tailored to the user’s selection of default promoters such as *OsU3*, *TaU3* and CmYLCV. Finally, the web server outputs all possible pegLs and pegRs, displaying details on the target sequence (5’–3’), PBS,

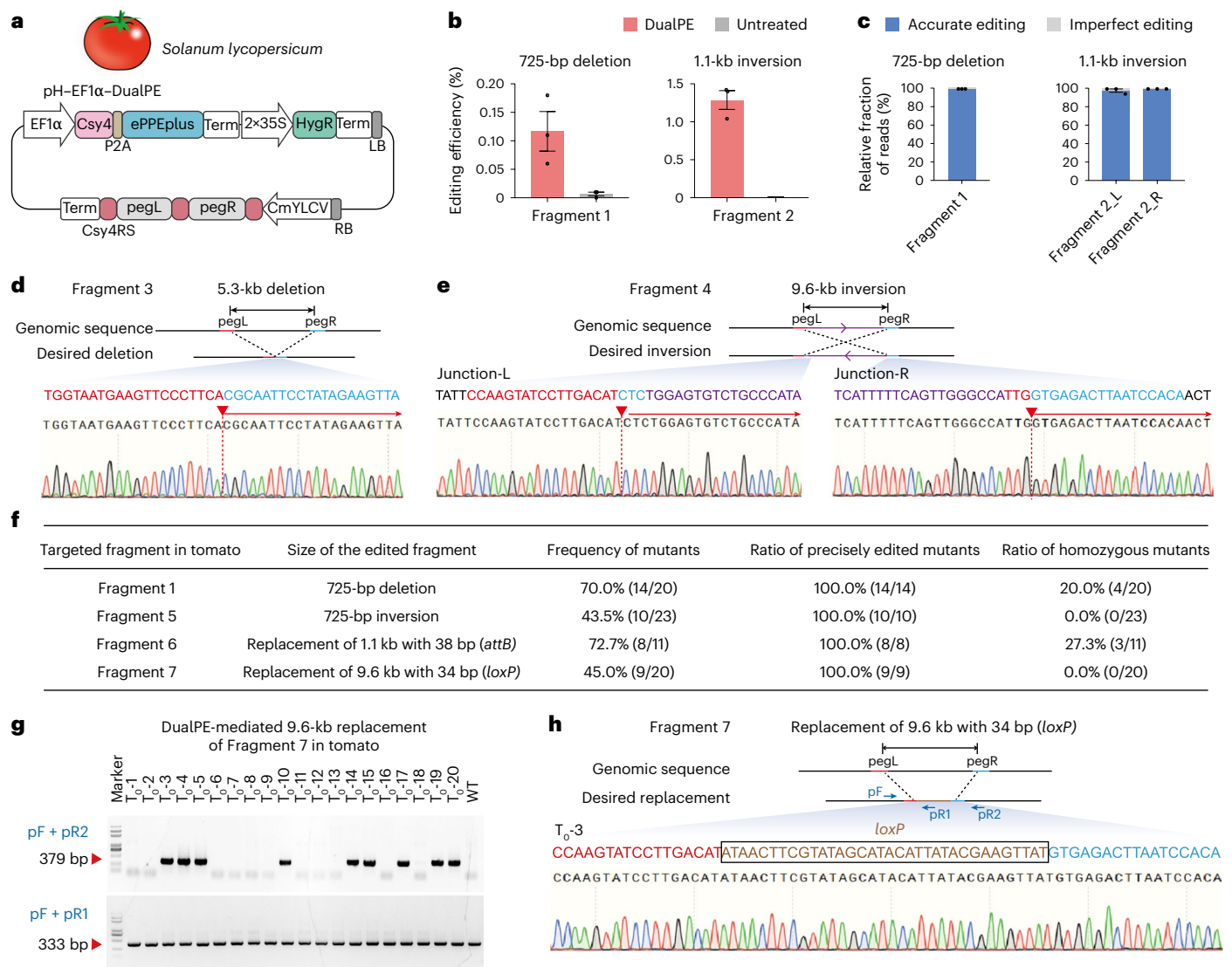


Fig. 6 | DualPE enables large DNA editing in tomato. a, Representation of the pH-EF1 α -DualPE construct used for tomato DNA editing. **b**, Frequency for the 725-bp deletion and 1.1-kb inversion at two endogenous loci induced by DualPE in tomato cells, as measured by dPCR. **c**, Fraction of reads with a precise deletion or inversion and imperfect editing. The editing rate represents the number of reads with the indicated editing/total editing events. The values and error bars in **b** and **c** represent means and standard errors of the mean of three independent biological replicates. **d, e**, Sanger sequencing chromatograms of the precise 5.3-kb deletion (**d**) and 9.6-kb inversion (**e**). The left protospacer, right

protospacer and inverted sequences are shown in red, blue and purple, respectively. **f**, Summary of DualPE-mediated edit frequencies for the 725-bp deletion, the 725-bp inversion, the replacement of 1.1 kb with 38 bp and the replacement of 9.6 kb with 34 bp in tomato plants. **g**, Representative agarose gel of PCR products for genotyping the replacement of 9.6 kb with 34 bp (Fragment 7). The 379-bp bands are the desired bands for the replacement, while the 333-bp bands are the size for the WT sequence. **h**, Sanger sequencing chromatograms of the precise 9.6-kb replacement with 34 bp. The desired replacements are shown in brown.

RTT, primers and the sequences after editing, which are recommended on the basis of the cumulative distance of pegL nicking from the desired start position and pegR nicking from the desired end position, specifically ranked from the shortest to the longest distance (Fig. 7a and Extended Data Fig. 10).

In summary, applying DualPE to achieve editing of large fragments in plants comprises several steps (Fig. 7b). First, dual pegRNAs are designed using DualPE-Finder, and vectors are constructed with the Gibson or Goldengate cloning method. Second, the efficiency and accuracy of large DNA editing events are assessed in a transient system such as protoplasts using polyethylene-glycol-mediated transfection or in leaves via *Agrobacterium*-mediated infiltration. For evaluating editing efficiency, high-throughput amplicon sequencing is recommended for edited fragments <200 bp and dPCR for edited fragments >200 bp; precision can be estimated by high-throughput amplicon

sequencing and Sanger sequencing for any range. Third, all DualPE components are delivered into plant cells via *Agrobacterium* or particle bombardment, followed by tissue culture and plant regeneration. Fourth, plants with the desired editing events are identified using PCR genotyping and verified by Sanger sequencing. The entire procedure may take four to five months.

Discussion

In the present study, we developed a PE-based genome editing approach, DualPE, which achieves efficient and scarless large DNA editing in wheat, *N. benthamiana* and tomato, including deletions, replacements and inversions, expanding the scope of genome editing in plants. We used epegRNAs and an optimized prime editor, ePPEplus, in our DualPE system to enhance efficiency. The epegRNA, featuring tevopreQ1 at its 3' end⁴⁴, showed a 3.0-fold increase in

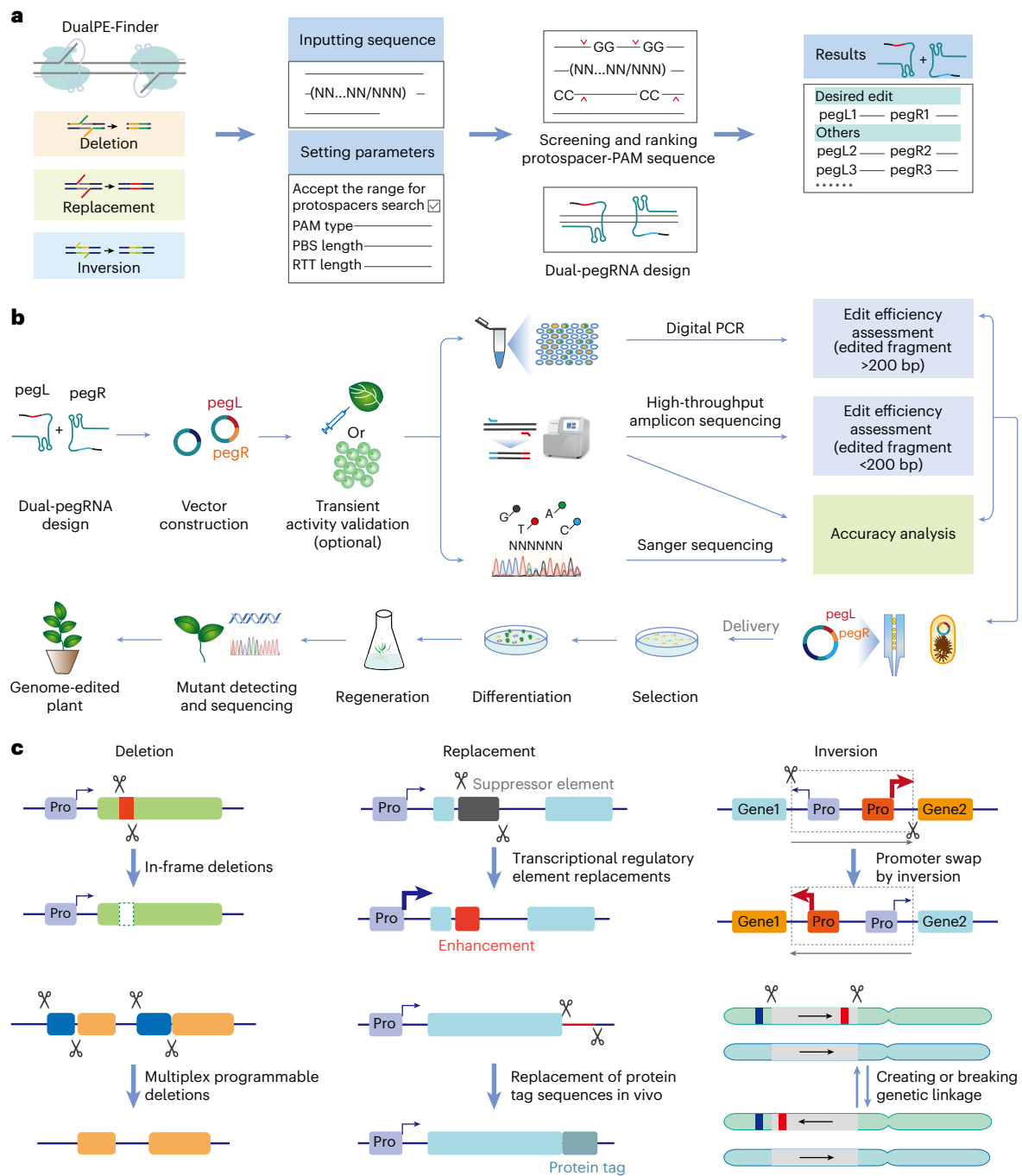


Fig. 7 | Pipeline and potential application of DualPE for editing large DNA fragments in plants. **a**, Workflow of DualPE-Finder for designing dual-pegRNA. DualPE-Finder allows users to input sequences in the required format and customize parameters. After submission, the web server identifies flanking protospacers and PAM sequences, designs pegRNAs and generates primers for the selected promoters. The resulting pegRNA candidates are ranked by their nicking distance from the target sites. **b**, General procedure for large DNA fragment editing in plants using DualPE. The main steps include designing dual-pegRNA on the DualPE-Finder web server, constructing dual-pegRNA,

evaluating the efficiency and accuracy of DualPE by dPCR, high-throughput amplicon sequencing and Sanger sequencing in a transient expression system, transforming and regenerating plants, and identifying plants carrying large DNA edits. **c**, Potential applications of DualPE. DualPE can be used for generating in-frame deletions and multiplexing programmable deletions. DualPE may also allow the replacement of genomic regions with other types of sequences, such as epitope tags, mini-promoters or other regulatory elements. DualPE can be further used to swap promoters, create new linkage groups or break linkage groups.

efficiency over standard pegRNAs in wheat cells³⁶. The ePPEplus editor, which we previously developed, includes the V223A mutation in RT and R221K and N394K mutations in nCas9 (H840A), along with optimized nuclear localization signals (NLSs), resulting in approximately 33.0-fold higher activity than the original prime editor in wheat cells³⁶. Thus, the combination of epegRNA and ePPEplus theoretically

further boosts the efficiency of DualPE-mediated large DNA editing in plants.

We first conducted a thorough comparative analysis of the editors DualPE, WT-DualPE and Cas9 for the introduction of deletions, which revealed that DualPE outperformed the other two systems in efficiency and precision for deletions ranging from -500 bp to -365.9 kb in wheat

protoplasts. The DualPE-mediated deletion approach is similar to those previously developed in human cells, such as PRIME-Del and twinPE, which can achieve deletions of up to 10 kb (the largest size tested)^{30,32}. Notably, our study demonstrates that DualPE can introduce deletions exceeding 10 kb, reaching up to 2 Mb in hexaploid wheat, thereby broadening the editing scope of PE. In contrast, WT-DualPE is similar to the PEDAR method, which can introduce >10-kb targeted deletions and 60-bp insertions in mammalian cells³¹. This process potentially uses mechanisms similar to the microhomology-mediated end joining pathway or the single-strand annealing pathway during the repair of the two DSBs³¹. Large DNA deletions mediated by Cas9 are primarily repaired by the non-homologous end-joining pathway for two DSBs. Hence, despite the capability of both WT-DualPE and Cas9 to induce deletions in wheat cells, the repair process of the two induced DSBs tends to be more prone to errors, ultimately yielding indel mutations at the junction site. DualPE, as illustrated in Fig. 1, circumvents the generation of DSBs and employs a distinct repair pathway for large DNA deletions. This may be a key reason for its ability to achieve more efficient and precise large deletions in plants than WT-DualPE and Cas9. In addition, we noticed that there is no strong relationship between deletion size and deletion efficiency across the seven sites we tested for each strategy, which is consistent with the findings in human cells³⁰. Beyond the activities of the pegRNAs or sgRNAs at the targeted sites (Supplementary Fig. 13), several other factors may contribute to this lack of correlation, including sequence context, copy number of target sites, chromatin environment, epigenetic modifications and spatial distance within the 3D chromosome structure of the targeted region, among others^{45,46}. It is intriguing to further explore the comprehensive impact of various factors on large-fragment editing efficiency, as well as to analyse editing characterization across different scales. The deletion method can further be employed to introduce in-frame deletions and multiplex programmable deletions by using multiple pairs of dual-pegRNA, thereby preventing the activation of the nonsense-mediated decay pathway and avoiding unintended deletions (Fig. 7c).

DualPE was effective for precise replacements of long sequences, including deletions of up to ~258 kb and insertions of up to 90 bp, with efficiencies of up to 43.0% in wheat protoplasts. DualPE displayed much higher editing efficiency than WT-DualPE for replacements. This observation is consistent with findings that GRAND (similar to DualPE) outperformed aPE (similar to WT-DualPE) in human cells³³, and that ePPE (similar to DualPE) demonstrated greater efficiency than ePPE-wtCas9 (similar to WT-DualPE) in rice cells²⁹. DualPE-mediated replacements can be used to modify gene expression, as shown in this study by concurrently deleting a 567-bp fragment and precisely replacing it with a 157-bp insertion at the *VRT-A2* locus; such combined deletion–insertion can be used to introduce other types of sequences^{37–40}, such as epitope tags, *cis*-elements or other regulatory elements (for example, mini-promoters) to manipulate the expression levels of agronomically important genes (Fig. 7c). In the future, increasing the RTT transcript length during the reverse transcription process could enhance the potential for DualPE-mediated larger replacements, enabling more extensive genomic modifications.

We used DualPE alone to invert DNA fragments ranging from 713 bp to ~252 kb with up to 51.5% efficiency in wheat protoplasts and plants. DualPE achieved more precise inversions by using nCas9 activity that operates independently of DSBs. As speculated in Fig. 1, two 3' DNA flap sequences of RTT anneal to the inverted region of their complementary sequence. This annealing acts as a primer to initiate DNA synthesis in the opposite orientation through DNA replication. This DNA repair mechanism may be similar to the recent AE system, which uses two pegRNAs for large DNA duplications³⁵. In contrast, WT-DualPE—similar to the PETI strategy used in human cells³⁴—and Cas9 introduce DSBs, which engage various repair pathways, potentially leading to unintended mutations (Supplementary Fig. 13). Importantly, precise promoter swapping can also be achieved using this

system, providing methods to regulate gene expression *in situ* without donor DNA. Besides swapping promoters, induced inversions can also be potentially used to create new linkage groups or break up linkage groups (Fig. 7c).

The recent combination of PE with recombinase (PE+recombinase) represents another advanced method for large DNA editing, which can achieve inversions and insertions of up to tens of kilobase pairs in human cells and plant cells^{29,32}. Compared with the PE+recombinase system, DualPE has several advantages in plants. One is simplicity of design: DualPE requires only two pegRNAs without the need for donor DNA, whereas PE+recombinase requires four pegRNAs and the recombinase for inversions, or two pegRNAs, the recombinase and donor DNA for insertions. A second advantage is scarless editing: DualPE does not leave a scar at the junctions, whereas PE+recombinase leaves recombination sites in the genome. A third is flexible delivery methods: the DualPE system features a much smaller vector and offers more flexibility in delivery methods, usually with a one-step transformation, whereas PE+recombinase (especially for insertions) is not suitable for using *Agrobacterium*-mediated transformation, which requires a two-step method due to requiring donor DNA and thus results in lower efficiency than particle bombardment²⁹.

On the basis of this study and our previous research^{36,47–49}, a prime editor can achieve different types and scales of editing. For example, when using one pegRNA, a prime editor can achieve one or several base substitutions as well as small indels; when using a dual-pegRNA system, targeting the opposite strands can achieve precise large deletions, replacements or inversions; and with multiple pegRNAs, the editing of multiple genomic sites that combines various mutations simultaneously is possible (Supplementary Fig. 14). In this study, we tested the effect of introducing the T128N, N200C and V223Y mutations of PE6d⁵⁰ into DualPE (DualPE-6d) to enhance PE activity for larger DNA fragments but observed no enhancing effect (Supplementary Fig. 15). Nonetheless, overall absolute editing efficiency, precision, targeting scope and the exact mechanisms of DualPE still need to be further understood and improved.

In summary, the DualPE approach presented in this study provides new avenues for precision chromosome editing in plants, enabling not only efficient and programmable deletion and replacement of large DNA fragments into target genomic loci, but also precise large inversions in both monocot and dicot plants. The simplicity and robustness of the method might enable the study of basic biology questions and support crop improvement arising from complex structural mutations.

Methods

Plasmid construction

The plasmid DualPE was identical to the previously reported CMPE-ePPEplus³⁶. The plasmid WT-DualPE restored the mutated Ala840 residue to the original His840 through mismatch PCR; the resulting coding sequence was cloned into the DualPE construct backbone. The Cas9 vector was constructed by amplifying Cas9 from the vector pBUE411 (ref. 51) and cloning it into pJIT163. The plasmid DualPE-6d was mutated via mismatch PCR to incorporate the T128N, N200C and V223Y mutations, with the resultant coding sequence cloned into the DualPE backbone. To construct the binary vector pB-DualPE for *A. tumefaciens*-mediated wheat transformation, the DualPE cassette and the dual-epgRNA array were cloned into pB-CMPE-ePPEplus³⁶. The T-DNA vectors pH-2×35S-DualPE and pH-EF1α-DualPE were constructed by replacing the *ZmUbi* promoter of pB-DualPE with the 2×35S promoter and *EF1α* promoter, respectively, and replacing the Basta-resistance gene (*Bar*) of pB-DualPE with hygromycin-resistance gene (*Hyg*). The dual epegRNAs were constructed into the pUC57-CmYLCV vector³⁶ through either Gibson or Goldengate cloning methods²⁶. To construct the esgRNA expression vectors, primers containing the target spacer were annealed and subsequently cloned into the TaU3-esgRNA backbone³⁶. PCR was

performed using 2× Phanta Max Master Mix (Nanjing Vazyme Biotech). A ClonExpressII One Step Cloning Kit (Nanjing Vazyme Biotech) was used for vector cloning. The primer sets used in this study are listed in Supplementary Table 4.

Wheat and tomato protoplast transfection

The spring wheat variety ‘Fielder’ and the tomato (*Solanum lycopersicum* L.) cultivar Micro-Tom were used to prepare protoplasts. The isolation and transfection of wheat and tomato protoplasts were conducted as described previously^{52,53}. For protoplast transfection, high-quality plasmids were purified through the Wizard Plus Midiprep DNA Purification System (Promega). Then, 5 µg of each plasmid was mixed and introduced into plant protoplasts via polyethylene-glycol-mediated transfection^{52,53}. The transfection efficiency was assessed using GFP as a control through microscopy, yielding approximately 30–60% for wheat and around 20–30% for tomato. During the protoplast transfection process, different treatments were performed side by side and in parallel, and the entire process was repeated three times (representing three biological replicates). After incubation at 25 °C for 48 h, the transformed protoplasts were collected by centrifugation for genomic DNA extraction^{52,53}.

Agrobacterium-mediated *N. benthamiana* infiltration

Leaves of *N. benthamiana* plants at the six-leaf stage were infiltrated with *Agrobacterium* cell suspensions containing binary plasmids. The *agrobacteria* (GV3101::pMP90 strain) were prepared from an overnight primary culture, followed by 6-h to 8-h secondary culture in LB medium supplemented with 100 mg l⁻¹ kanamycin and 30 mg l⁻¹ rifampicin. The *Agrobacterium* cells were collected by centrifugation; resuspended in a buffer containing 10 mM MgCl₂, 10 mM MES monohydrate (pH 5.7) and 200 µM acetosyringone to achieve an optical density at 600 nm of 0.8; and incubated for 2–3 h before infiltration⁵⁴. At 3 d post-infiltration, the infiltrated zones were collected, and total genomic DNA was isolated using the cetyltrimethyl ammonium bromide (CTAB) method.

High-throughput amplicon sequencing

For next-generation sequencing, the target sites were amplified from protoplast genomic DNA using site-specific primers in the first round of PCR. In the second round, forward and reverse barcodes were added to the PCR products for library construction³⁶. The amplified products were purified using a Universal Micro DNA Cleanup and Concentrate Kit (Aidlab) and quantified with a NanoDrop 2000 spectrophotometer (Thermo Fisher Scientific)³⁶. Equal amounts of PCR products were pooled and commercially sequenced (GENEWIZ) using the NovaSeq platform. For each target locus, amplicon sequencing was performed three times using genomic DNA extracted from three independent protoplast samples³⁶. The analysis of editing efficiencies for replacement (defined as an amplicon length difference of <200 bp between the WT and edited DNA products) was performed with custom shell scripts²⁶. The primers used are listed in Supplementary Table 4.

Accuracy analysis

High-throughput amplicon sequencing was used to evaluate the accuracy of any range of DNA editing with custom shell scripts⁵⁵. For deletions and inversions, the frequency of accurate indicated editing was calculated as: percentage (number of reads with completely accurate editing without by-products) / (number of total reads). The frequency of imperfect indicated editing was calculated as: percentage (number of reads with indicated editing but not completely precise) / (number of total reads)³¹. For replacements, the frequency of accurate replacement was calculated as: percentage (number of reads with accurate replacement without by-products) / (number of total reads). The frequency of imperfect replacement was calculated as: percentage (number of reads with replacements containing at least half of the inserted fragment but not the precise insertion) / (number of total reads)²⁹. The frequency of

direct deletion was calculated as: percentage (number of reads with indels with direct deletion but neither precise nor imprecise insertions) / (number of total reads).

Digital PCR assay

Specific primers and TaqMan probes for deletion junctions, inserted sequences and inverted sequences were designed and are listed in Supplementary Table 2. The probe for the endogenous control was detected using the HEX fluorescence channel, while the edited events were detected using the FAM fluorescence channel²⁹. The reaction mixtures contained 200 ng of wheat genomic DNA, 0.8 µM of each primer, 0.4 µM of each probe, 10 µl of 4× Probe PCR Master Mix for Probes (QIAGEN) and water to a final volume of 40 µl. The reaction mixtures were transferred into QIAcuity Nanoplate 26k 24-well plates (QIAGEN) and covered by a membrane. Digital PCR was performed under the following conditions: 95 °C for 2 min and 40 cycles of 95 °C for 15 s and 59 °C for 30 s. The digital signals were read using a QIAcuity One, Splex Device (QIAGEN), and the data were analysed with the QIAcuity Software Suite (v.2.5.0.1).

Agrobacterium-mediated transformation of wheat and tomato

The binary plasmid pB-DualPE containing the dual-epgRNA array was transformed into *A. tumefaciens* strain EHA105. *Agrobacterium*-mediated transformation of immature embryos of the wheat variety ‘Fielder’ was conducted according to Kumar et al.⁵⁶. The binary plasmid pH-EF1α-DualPE containing the dual-epgRNA array was transformed into *A. tumefaciens* strain GV3101. *Agrobacterium*-mediated transformation of the cotyledons from *S. lycopersicum* (L.) cv. Alisa Craig was conducted according to Van Eck et al.⁵⁷.

Genotyping of transgenic plants

Genomic DNA from wheat and tomato plants was extracted using a 2× CTAB solution (Coolaber) and PCR-amplified with 2× Phanta Max using universal primers and/or specific primers that spanned the target sites⁵². The resulting PCR products were analysed via agarose gel electrophoresis and validated through Sanger sequencing⁵². To genotype the deletion and replacement mutants for edited fragments <2 kb, specific primers (pF + pR) flanking the two target sites were used to amplify the desired sequence. Mutants can be amplified with only one band (shorter, homozygous mutation) or two bands (one longer and one shorter, heterozygous or chimeric mutation). To genotype the deletion and replacement mutants for edited fragments >2 kb, PCR used two pairs of specific primers, one pair (pF + pR1) to amplify the WT sequence and another (pF + pR2) for the deleted or replaced sequence. Mutants can be amplified with only pF + pR2 (homozygous mutation) or with both pF + pR1 and pF + pR2 (heterozygous or chimeric mutation). To genotype the inversion mutants, PCR used four pairs of specific primers, one pair (L_pF + R_pF) to amplify the inversion Junction-L sequence, another (L_pR + R_pR) for the inversion Junction-R sequence and another two pairs of primers (L_pF + L_pR and R_pF + R_pR) to amplify the WT genomic region. Mutants can be amplified with only L_pF + R_pF and L_pR + R_pR (homozygous mutation) or with all four pairs of primers (heterozygous or chimeric mutation). DNA from each mutant was extracted from independent leaves at least three times. The primers for mutant identification are listed in Supplementary Table 4.

RNA extraction and qRT-PCR

For the qRT-PCR assays, wheat glumes at the heading stage were collected for *VRT-A2*, and the fifth leaf sheath at the jointing stage was collected for wheat Fragment 23. Total RNA was extracted using TRIzol reagent (Thermo Fisher Scientific) following the manufacturer’s instructions. After the removal of genomic DNA, cDNAs were synthesized using a Reverse Transcription kit (Vazyme). Quantitative PCR was carried out using SYBR Green PCR Master Mix (Vazyme) on a CFX96 Real-Time PCR System (Bio-Rad)³⁷. The wheat *ACT1N*

gene (TraesFLD5D01G146100) and the *CYCLIN-T1-3* gene (TraesFLD2A01G379900) served as internal controls in the qRT-PCR analysis for the *VRT-A2* gene and the wheat Fragment 23, respectively. Each experiment was performed three times. The primers used for the qRT-PCR assays are listed in Supplementary Table 4.

Trait evaluation

The wheat materials were grown in a greenhouse at 24 °C under a 16-h light/8-h dark photoperiod or in the experimental field of China Agricultural University in Beijing under normal water and fertilizer conditions. Homozygous T₁ plants were used to evaluate the traits. Ten independent wheat plants were selected, and spikelets in the middle part of the main spikes were analysed. The glume lengths, grain lengths and grain widths were measured using an automatic seed size analysing system (SC-G, Wanshen)³⁷.

Web server for dual-pegRNA design

To design dual-pegRNA sequences, we developed a Python-based web server, called DualPE-Finder, that accepts both direct sequence inputs and FASTA formatted files, enabling precise customization of sequence edits for deletions, replacements and inversions.

Deletions within the sequence are clearly indicated in parentheses and followed by a slash, '(a/)', where 'a' represents the sequence to be deleted. For example, 'AATCTTTCAGCGTTGGGTCAATCTCGTATATTTCTGCCATCTCCTGGT(TTTGGGACAACCTCGCGTTTCTCCCCACG...CAAGTCGTCGCTCTCACCGTCAGGCACCAGGA/)CCTTCCCTGGA GAGGCCGCGCGCTCAGGACGGCGCTGCAATGCAAGGA' demonstrates a deletion with parts of the sequence omitted for simplicity. The result will cause 'TTTGGGACAACCTCGCGTTTCTCCCCACG...CAAGTCGTCGCTCTCACCGTCAGGCACCAGGA' to be precisely deleted.

Replacements are denoted by '(a/b)', where 'a' is replaced with 'b'. An example is 'ACGCGTGAGAGGCAGGCATTCGTTGCAGCTCCCTCTAGAAATGCCCA(TCCTGGTGGATTTTCTTGCTGTTGCT...CTTACATGACTGGTAGTAGTGCCTTCCCAGT/TACCCATACGATGTTCCTGACTATGCGGGTACTCCCTATGACTCCCGGACTATGACTATGACTCCATCATATGACGTTCCAGATTACGCT)CTTTGACATGTTCCGCCGACCGTGCAACATTGCTGGTGAAGCATGGGTG'. The result will cause 'TCCTGGTGGATTTTCTTGCTGTTGCT...CTTACATGACTGGTAGTAGTGCCTTCCCAGT' to be precisely replaced with 'TACCCATACGATGTTCCGACTATGCGGGTACTCCCTATGACTCCCGGACTATGAGGATCCTATCCATATGACGTTCCAGATTACGCT'.

Inversions within the sequence are indicated by the notation '(a)', where 'a' is the sequence to be inverted. An example is 'CGCCACCTGCCTCTGCGTGCCCGGGCACCTACGGCAACAAGGGCGCTGCCCTGCTAC AACAAGTGAAGACCAAGGAGGGAGGCCCAAGTGCCCTAGATTTCT(TGGTTTTCTTCTTCTTCTTCTTCTTCTTCTTGGGGTGCCAGCTTGGGTTGATGGCTATTACTG...ACGGATGTGATCCAGAGAAAAGGGCCCGGCAAACCGCGGATGACCGGGGGCTCTGCATTATCAACCC)TACGCAGACACAGACAGCGCAATGGCGACCAAGGATAGCACCGCGAGCCTGTTCCACAAGAAGCTGTTGGGCAGGGCCGGTAGGC'. The result will cause 'TGGTTTTCTTCTTCTTCTTCTTCTTCTTCTTGGGGTGCCAGCTT-GCGGTTGATGGCTATTACTG...ACGGATGTGATCCAGAGAAAAGGGC-CGGCAAACCGCGGATGACCGGGGGCTCTGCATTATCAACCC' to be precisely inverted.

The ellipsis '...' is optional, used to indicate portions of the sequence that are intentionally omitted for brevity. When using an ellipsis, the lengths between the ellipsis and the parentheses must exceed the values set by the 'Accept the range for protospacers search' sub-options.

The web server provides several PAM types, including SpCas9's NGG and its variants NGN, NRN and NYN. The web server searches for protospacers and PAMs located near the targeted editing sites. However, the nicking sites induced by DualPE may not always align perfectly with the desired editing location. In such scenarios, the web server offers the 'Accept the range for protospacers search' option, selected by

default, which expands the search around both the starting and ending positions of the intended editing fragment. This expansion is based on the user-specified regions ('Region for nick of pegL from the desired start position' and 'Region for nick of pegR from the desired end position'), set to extend on both sides, effectively extending the specified length in search of suitable PAM sequences. This flexibility increases the chances of successful editing by accommodating variations in the PAM location. If this option is unchecked, the system designs pegRNAs to strictly match the specified genomic location. Additionally, the web server comes with a range of adjustable parameters that are preset to default values, offering users the flexibility to modify them as needed for their specific projects. These parameters include Tm-directed PBS length model (selected by default), recommended Tm of PBS sequence at 30 °C (32 °C is recommended if 30 °C is not possible), PBS length set to 7–16 bp (default) and RTT length. For deletions and inversions, the RTT length functions as the homology arm, which is essential for aligning with the target site to facilitate the intended genomic modifications (the default is 30 bp). In the case of replacements, this length is termed 'Homology overlap between pegL and pegR', defining the overlap between the 3' extension of two pegRNAs to ensure accurate sequence insertion. It offers the option to exclude the first C in the RTT by default. The program also facilitates primer design, with the default promoters OsU3, TaU3 and CmYLCV available for users, employing the Gibson method for vector construction.

The output includes detailed information on target sequence (5'–3'), PBS sequence (length and Tm value), RTT sequence (length) and nick-to-desired-start/end edit distance. Primer designs are also included in the output for user convenience. Additionally, the output contains the sequences after editing, providing users with a comprehensive view of the anticipated genomic modifications. The website is now available at http://wheat.cau.edu.cn/DualPE_Finder/.

Statistics and reproducibility

All experiments were carried out in triplicate at least. We used GraphPad Prism v.8.0.1 to analyse the data. All numerical values are presented as mean ± s.e.m. Differences between the control and treatments were tested using two-tailed Student's *t*-tests.

Reporting summary

Further information on research design is available in the Nature Portfolio Reporting Summary linked to this article.

Data availability

DNA sequencing data have been deposited in the National Center for Biotechnology Information Sequence Read Archive database with the BioProject accession code [PRJNA1192508](https://www.ncbi.nlm.nih.gov/bioproject/PRJNA1192508). For data visualization, we used GraphPad Prism v.8.0.1, Microsoft Excel 2021, PowerPoint 2021 and Adobe Illustrator 2020. Source data are provided with this paper.

Code availability

The source code for DualPE-Finder is available at <https://github.com/ZongyuanLab/DualPE>. An interactive web page for designing dual-pegRNA for DualPE is available at http://wheat.cau.edu.cn/DualPE_Finder/.

References

1. Tao, Y., Zhao, X., Mace, E., Henry, R. & Jordan, D. Exploring and exploiting pan-genomics for crop improvement. *Mol. Plant* **12**, 156–169 (2019).
2. Zhao, J. et al. Genome-wide association study reveals structural chromosome variations with phenotypic effects in wheat (*Triticum aestivum* L.). *Plant J.* **112**, 1447–1461 (2022).
3. Yuan, Y., Bayer, P. E., Batley, J. & Edwards, D. Current status of structural variation studies in plants. *Plant Biotechnol. J.* **19**, 2153–2163 (2021).

4. Hu, H. et al. Unravelling inversions: technological advances, challenges, and potential impact on crop breeding. *Plant Biotechnol. J.* **22**, 544–554 (2023).
5. Gao, C. Genome engineering for crop improvement and future agriculture. *Cell* **184**, 1621–1635 (2021).
6. Zhou, X. et al. CRISPR-mediated acceleration of wheat improvement: advances and perspectives. *J. Genet. Genomics* **50**, 815–834 (2023).
7. Puchta, H. & Houben, A. Plant chromosome engineering—past, present and future. *New Phytol.* **241**, 541–552 (2023).
8. Huang, T. K. & Puchta, H. Novel CRISPR/Cas applications in plants: from prime editing to chromosome engineering. *Transgenic Res.* **30**, 529–549 (2021).
9. Jinek, M. et al. A programmable dual-RNA-guided DNA endonuclease in adaptive bacterial immunity. *Science* **337**, 816–821 (2012).
10. Cong, L. et al. Multiplex genome engineering using CRISPR/Cas systems. *Science* **339**, 819–823 (2013).
11. Li, S. et al. Genome-edited powdery mildew resistance in wheat without growth penalties. *Nature* **602**, 455–460 (2022).
12. Wang, Y. et al. Deletion of a target gene in Indica rice via CRISPR/Cas9. *Plant Cell Rep.* **36**, 1333–1343 (2017).
13. Cai, Y. et al. CRISPR/Cas9-mediated deletion of large genomic fragments in soybean. *Int. J. Mol. Sci.* **19**, 3835 (2018).
14. Tan, J. et al. Efficient CRISPR/Cas9-based plant genomic fragment deletions by microhomology-mediated end joining. *Plant Biotechnol. J.* **18**, 2161–2163 (2020).
15. Zhou, H., Liu, B., Weeks, D. P., Spalding, M. H. & Yang, B. Large chromosomal deletions and heritable small genetic changes induced by CRISPR/Cas9 in rice. *Nucleic Acids Res.* **42**, 10903–10914 (2014).
16. Schwartz, C. et al. CRISPR–Cas9-mediated 75.5-Mb inversion in maize. *Nat. Plants* **6**, 1427–1431 (2020).
17. Schmidt, C. et al. Changing local recombination patterns in *Arabidopsis* by CRISPR/Cas mediated chromosome engineering. *Nat. Commun.* **11**, 4418 (2020).
18. Schmidt, C., Pacher, M. & Puchta, H. Efficient induction of heritable inversions in plant genomes using the CRISPR/Cas system. *Plant J.* **98**, 577–589 (2019).
19. Lu, Y. et al. A donor-DNA-free CRISPR/Cas-based approach to gene knock-up in rice. *Nat. Plants* **7**, 1445–1452 (2021).
20. Ronspies, M. et al. Massive crossover suppression by CRISPR–Cas-mediated plant chromosome engineering. *Nat. Plants* **8**, 1153–1159 (2022).
21. Liu, J., Wang, F. Z., Li, C., Li, Y. & Li, J. F. Hidden prevalence of deletion–inversion bi-alleles in CRISPR-mediated deletions of tandemly arrayed genes in plants. *Nat. Commun.* **14**, 6787 (2023).
22. Beying, N., Schmidt, C., Pacher, M., Houben, A. & Puchta, H. CRISPR–Cas9-mediated induction of heritable chromosomal translocations in *Arabidopsis*. *Nat. Plants* **6**, 638–645 (2020).
23. Samach, A. et al. CRISPR/Cas9-induced DNA breaks trigger crossover, chromosomal loss, and chromothripsis-like rearrangements. *Plant Cell* **35**, 3957–3972 (2023).
24. Wang, M. et al. Gene targeting by homology-directed repair in rice using a geminivirus-based CRISPR/Cas9 system. *Mol. Plant* **10**, 1007–1010 (2017).
25. Lu, Y. et al. Targeted, efficient sequence insertion and replacement in rice. *Nat. Biotechnol.* **38**, 1402–1407 (2020).
26. Anzalone, A. V. et al. Search-and-replace genome editing without double-strand breaks or donor DNA. *Nature* **576**, 149–157 (2019).
27. Vu, T. V., Nguyen, N. T., Kim, J., Hong, J. C. & Kim, J. Y. Prime editing: mechanism insight and recent applications in plants. *Plant Biotechnol. J.* **22**, 19–36 (2024).
28. Vats, S., Kumar, J., Sonah, H., Zhang, F. & Deshmukh, R. Prime editing in plants: prospects and challenges. *J. Exp. Bot.* **16**, erae053 (2024).
29. Sun, C. et al. Precise integration of large DNA sequences in plant genomes using PrimeRoot editors. *Nat. Biotechnol.* **42**, 316–327 (2023).
30. Choi, J. et al. Precise genomic deletions using paired prime editing. *Nat. Biotechnol.* **40**, 218–226 (2022).
31. Jiang, T., Zhang, X. O., Weng, Z. & Xue, W. Deletion and replacement of long genomic sequences using prime editing. *Nat. Biotechnol.* **40**, 227–234 (2022).
32. Anzalone, A. V. et al. Programmable deletion, replacement, integration and inversion of large DNA sequences with twin prime editing. *Nat. Biotechnol.* **40**, 731–740 (2022).
33. Wang, J. et al. Efficient targeted insertion of large DNA fragments without DNA donors. *Nat. Methods* **19**, 331–340 (2022).
34. Kweon, J. et al. Targeted genomic translocations and inversions generated using a paired prime editing strategy. *Mol. Ther.* **31**, 249–259 (2023).
35. Zhang, R. et al. Amplification editing enables efficient and precise duplication of DNA from short sequence to megabase and chromosomal scale. *Cell* **187**, 3936–3952 (2024).
36. Ni, P. et al. Efficient and versatile multiplex prime editing in hexaploid wheat. *Genome Biol.* **24**, 156 (2023).
37. Liu, J. et al. Ectopic expression of *VRT-A2* underlies the origin of *Triticum polonicum* and *Triticum petropavlovskyi* with long outer glumes and grains. *Mol. Plant* **14**, 1472–1488 (2021).
38. Adamski, N. M. et al. Ectopic expression of *Triticum polonicum* *VRT-A2* underlies elongated glumes and grains in hexaploid wheat in a dosage-dependent manner. *Plant Cell* **33**, 2296–2319 (2021).
39. Chai, S. Y. et al. Identification and validation of a major gene for kernel length at the *P1* locus in *Triticum polonicum*. *Crop J.* **10**, 387–396 (2022).
40. Xiao, J. et al. A natural variation of an SVP MADS-box transcription factor in *Triticum petropavlovskyi* leads to its ectopic expression and contributes to elongated glume. *Mol. Plant* **14**, 1408–1411 (2021).
41. Jiang, Y. Y. et al. Prime editing efficiently generates W542L and S621I double mutations in two *ALS* genes in maize. *Genome Biol.* **21**, 257 (2020).
42. Ma, S. et al. WheatOmics: a platform combining multiple omics data to accelerate functional genomics studies in wheat. *Mol. Plant* **14**, 1965–1968 (2021).
43. Niu, Q. et al. Efficient A.T to G.C base conversions in dicots using adenine base editors expressed under the tomato *EF1a* promoter. *Plant Biotechnol. J.* **21**, 5–7 (2023).
44. Nelson, J. W. et al. Engineered pegRNAs improve prime editing efficiency. *Nat. Biotechnol.* **40**, 402–410 (2022).
45. Liu, G., Yin, K., Zhang, Q., Gao, C. & Qiu, J. L. Modulating chromatin accessibility by transactivation and targeting proximal dsRNAs enhances Cas9 editing efficiency in vivo. *Genome Biol.* **20**, 145 (2019).
46. Li, X. et al. Chromatin context-dependent regulation and epigenetic manipulation of prime editing. *Cell* **187**, 2411–2427 e2425 (2024).
47. Lin, Q. et al. Prime genome editing in rice and wheat. *Nat. Biotechnol.* **38**, 582–585 (2020).
48. Lin, Q. et al. High-efficiency prime editing with optimized, paired pegRNAs in plants. *Nat. Biotechnol.* **39**, 923–927 (2021).
49. Zong, Y. et al. An engineered prime editor with enhanced editing efficiency in plants. *Nat. Biotechnol.* **40**, 1394–1402 (2022).
50. Doman, J. L. et al. Phage-assisted evolution and protein engineering yield compact, efficient prime editors. *Cell* **186**, 3983–4002 e3926 (2023).
51. Xing, H. L. et al. A CRISPR/Cas9 toolkit for multiplex genome editing in plants. *BMC Plant Biol.* **14**, 327 (2014).

52. Wang, Y. et al. Simultaneous editing of three homoeoalleles in hexaploid bread wheat confers heritable resistance to powdery mildew. *Nat. Biotechnol.* **32**, 947–951 (2014).
53. Randall, L. B. et al. Genome- and transcriptome-wide off-target analyses of an improved cytosine base editor. *Plant Physiol.* **187**, 73–87 (2021).
54. Hamel, L. P. et al. Molecular responses of agroinfiltrated *Nicotiana benthamiana* leaves expressing suppressor of silencing P19 and influenza virus-like particles. *Plant Biotechnol. J.* **22**, 1078–1100 (2024).
55. Komor, A. C., Kim, Y. B., Packer, M. S., Zuris, J. A. & Liu, D. R. Programmable editing of a target base in genomic DNA without double-stranded DNA cleavage. *Nature* **533**, 420–424 (2016).
56. Kumar, R. et al. Optimization of *Agrobacterium*-mediated transformation in spring bread wheat using mature and immature embryos. *Mol. Biol. Rep.* **46**, 1845–1853 (2019).
57. Van Eck, J., Keen, P. & Tjahjadi, M. *Agrobacterium tumefaciens*-mediated transformation of tomato. *Methods Mol. Biol.* **1864**, 225–234 (2019).

Acknowledgements

We thank C. Gao (Institute of Genetics and Developmental Biology, Chinese Academy of Sciences) for suggestions on the manuscript. This work was supported by grants from the National Key Research and Development Program of China (no. 2021YFF1000800 to Y. Zong, no. 2022YFF1002801 to Y.W. and no. 2023YFD1202904 to L.C.), the Biological Breeding-Major Projects (no. 2023ZD0407403 to Y.W.), the National Natural Science Foundation of China (no. 32270429 to Y. Zong and no. 32122051 to Y.W.) and the Chinese Universities Scientific Fund (no. 2024TC162 to Y. Zong).

Author contributions

Y. Zong, Y.W. and Y. Zhao designed the project. Y. Zhao, Z.H., X.Z., W.T., Z.L., Wenping Wang, S.T. and Y.L. performed the experiments. Y. Zong, Y.W. and Y. Zhao wrote the manuscript. Jing Liu, Wenxi Wang, L.C., N.Z., W.G., Jie Liu, Z.N. and Q.S. contributed to the discussion and revised the manuscript. Y. Zong and Y.W. supervised the project.

Competing interests

Y. Zong, Y.W., Q.S., Z.N. and Y. Zhao have submitted a provisional patent application (patent application no. 2024117368334, Republic of China) based on the results reported in this paper through China Agricultural University. The remaining authors declare no competing interests.

Additional information

Extended data is available for this paper at <https://doi.org/10.1038/s41477-024-01898-3>.

Supplementary information The online version contains supplementary material available at <https://doi.org/10.1038/s41477-024-01898-3>.

Correspondence and requests for materials should be addressed to Yanpeng Wang or Yuan Zong.

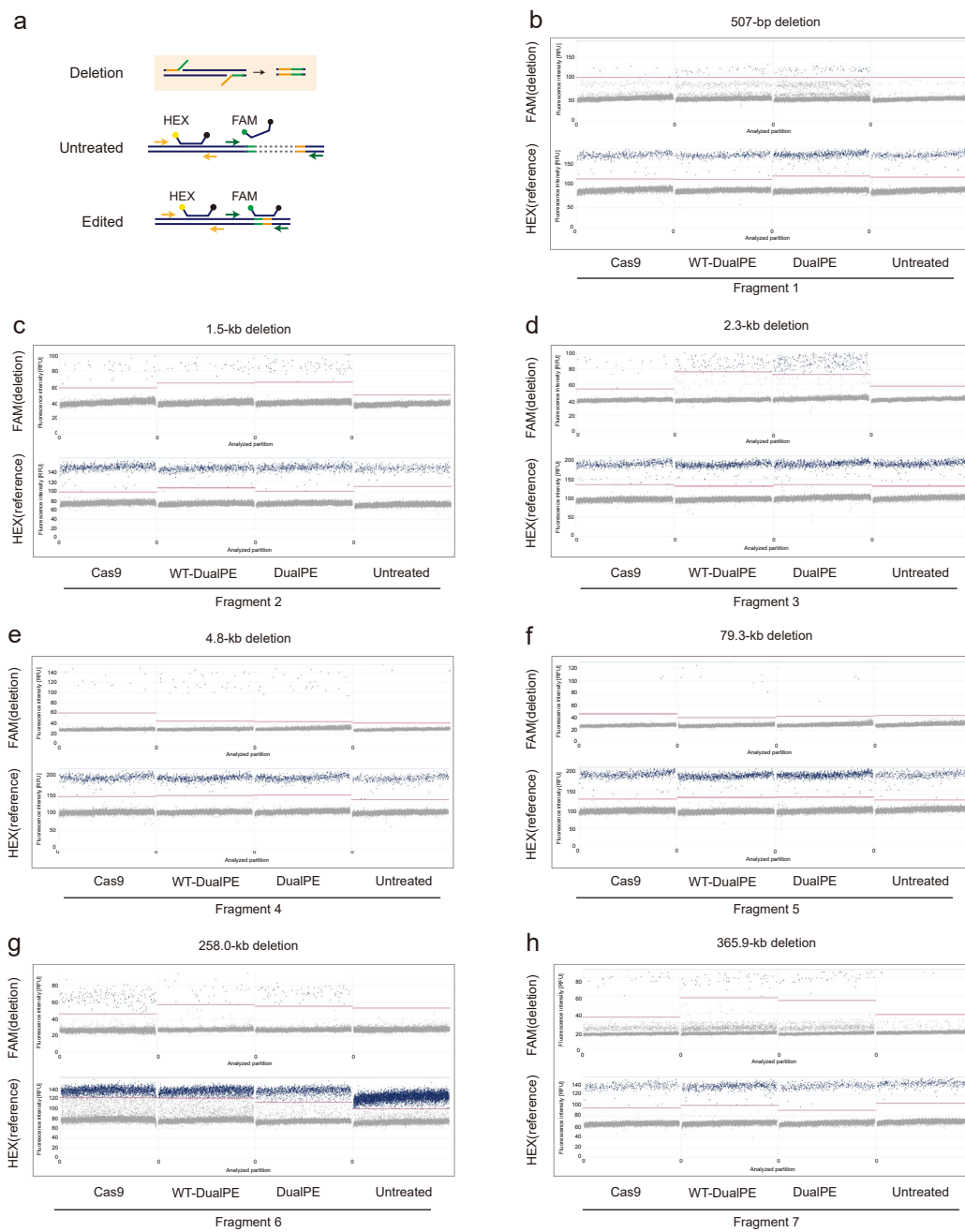
Peer review information *Nature Plants* thanks Sergei Svitashv and the other, anonymous, reviewer(s) for their contribution to the peer review of this work.

Reprints and permissions information is available at www.nature.com/reprints.

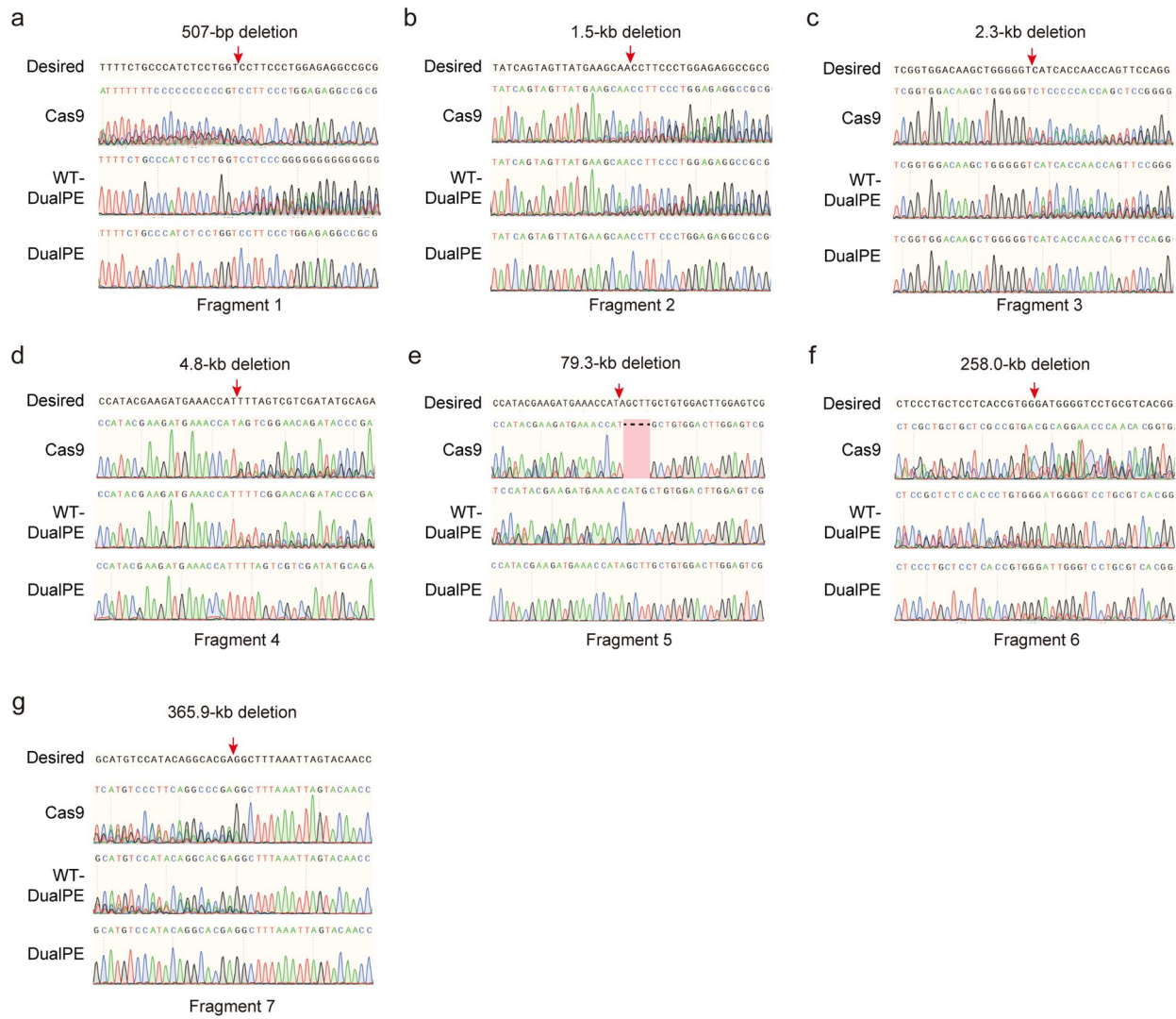
Publisher's note Springer Nature remains neutral with regard to jurisdictional claims in published maps and institutional affiliations.

Springer Nature or its licensor (e.g. a society or other partner) holds exclusive rights to this article under a publishing agreement with the author(s) or other rightsholder(s); author self-archiving of the accepted manuscript version of this article is solely governed by the terms of such publishing agreement and applicable law.

© The Author(s), under exclusive licence to Springer Nature Limited 2025

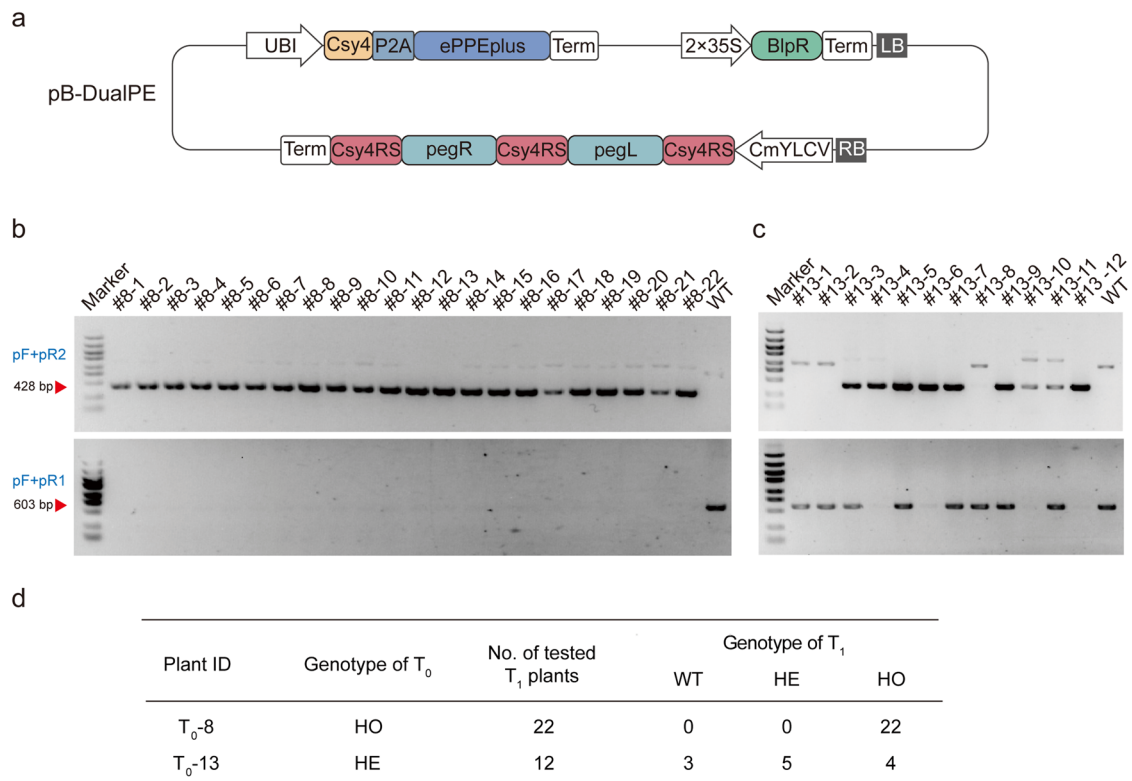


Extended Data Fig. 1 | dPCR results for detection of large DNA deletion in wheat protoplasts. a, Scheme of the dPCR assay for quantification of deletion events. **b-h**, Digital fluorescence level in dPCR assay for 507-bp deletion (b), 1.5-kb deletion (c), 2.3-kb deletion (d), 4.8-kb deletion (e), 79.3-kb deletion (f), 258.0-kb deletion (g) and 365.9-kb deletion (h).



Extended Data Fig. 2 | Sanger sequencing chromatograms of deletions induced by Cas9, WT-DualPE and DualPE in wheat protoplasts. a-g. Represented Sanger sequencing chromatograms for 507-bp deletion (a),

1.5-kb deletion (b), 2.3-kb deletion (c), 4.8-kb deletion (d), 79.3-kb deletion (e), 258.0-kb deletion (f) and 369.5-kb deletion (g). Red arrows represent the junction of two cut/nick sites.

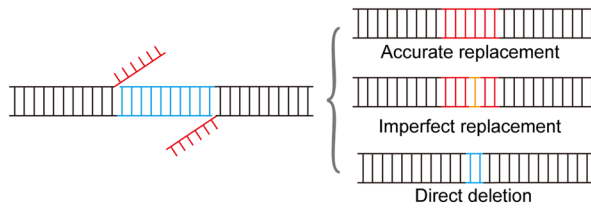


Extended Data Fig. 3 | Identification and analysis of the wheat mutants for 365.9-kb deletion. **a**, Schematic representation of the expression vector pB-DualPE for *Agrobacterium* transformation. **b,c**, Gel electrophoresis of PCR products for 365.9-kb deletion in T_1 generation of T_0 -8 (**b**) and T_0 -13 (**c**) line. The 428-bp band is the desired size for the deletion, while the 603-bp band is the

expected size for the wild-type sequence. WT, wild-type control plant.

d, Segregation analysis of T_0 -8 and T_0 -13 lines derived from DualPE-mediated 365.9-kb deletions of wheat plants. HO, homozygous; HE, heterozygous; WT, wild-type.

a



b

Fragment 9 Replacement of 60 bp with 38 bp (*attB*): WT-DualPE

Wild type	GGCCGATGCCGGTGC	CGGGCAGCGAGGAGT	---	AAGGCCTTCATCCTC	ACCATCACCAACCAG	
Desired	GGCCGATGCCGGT	ATGATCCTGACGACGGAGACCGCCGTCGT	CGACAAGCC	CCATCACCAACCAG		
Accurate replacement	GGCCGATGCCGGT	ATGATCCTGACGACGGAGACCGCCGTCGT	CGACAAGCC	CCATCACCAACCAG		80382/138686
Imperfect replacement	GGCCGATGCCGGT	ATGATCCTGACGACGGAGA	---	---	CCATCACCAACCAG	1561/138686
Direct deletion	GGCCGATGCCGGT	A	---	---	GGCCATCACCAACCAG	12013/138686
	GGCCGATGCCGGT	ATGAT	---	---	CCATCACCAACCAG	6691/138686
	GGCCGATGCCGGT	A	---	AGCC	CCATCACCAACCAG	5328/138686
	GGCCGATGCCGGT	A	---	---	TACCAACCAG	5230/138686
	GGCCGATGCCGG	---	---	---	CCATCACCAACCAG	3710/138686

Fragment 9 Replacement of 60 bp with 38 bp (*attB*): DualPE

Wild type	GGCCGATGCCGGTGC	CGGGCAGCGAGGAGT	---	AAGGCCTTCATCCTC	ACCATCACCAACCAG	
Desired	GGCCGATGCCGGT	ATGATCCTGACGACGGAGACCGCCGTCGT	CGACAAGCC	CCATCACCAACCAG		
Accurate replacement	GGCCGATGCCGGT	ATGATCCTGACGACGGAGACCGCCGTCGT	CGACAAGCC	CCATCACCAACCAG		52981/57455
Imperfect replacement	GGCCGATGCCGGT	ATGCTCCTGACGACGGAGACCGCCGTCGT	CGACAAGCC	CCATCACCAACCAG		577/57455
Direct deletion	GGCCGATGCCGGT	---	---	---	AGCCCATCACCAACCAG	1752/57455
	GGCCGATGCCGGT	---	---	AT	GCCCATCACCAACCAG	542/57455
	GGCCGATGCCGGT	---	---	AGCC	CCATCACCAACCAG	516/57455

c

Fragment 13 Replacement of 4.8 kb with 34 bp (*lox76*): WT-DualPE

Wild type	CGAAGATGAAACCAT	AGTCGGAACAGATAC	---	CTAAACCTCCCTCGCTTT	AGTCGTCGATAT	
Desired	CGAAGATGAAACCAT	ATAACTTCGTATAGCATACATTATACGCCGGT	ATTTAGTCGTCGATAT			
Accurate replacement	CGAAGATGAAACCAT	ATAACTTCGTATAGCATACATTATACGCCGGT	ATTTAGTCGTCGATAT			15798/57668
Imperfect replacement	CGAAGATGAAACCAT	ATAACTTCGTATAGCATACATTATACGCCGGT	ATTTAGTCGTCGATAT			12/57668
Direct deletion	CGAAGATGAAACCAT	ATAA	---	---	TTTAGTCGTCGATAT	7212/57668
	CGAAGATGAAACCAT	ATAA	---	---	TTTAGTCGTCGATAT	5872/57668
	CGAAGATGAAACCAT	ATAACT	---	---	TTTAGTCGTCGATAT	5436/57668
	CGAAGATGAAACCAT	ATAACT	---	---	TTTAGTCGTCGATAT	5011/57668
	CGAAGATGAAACCAT	ATAA	---	---	TTTAGTCGTCGATAT	4960/57668

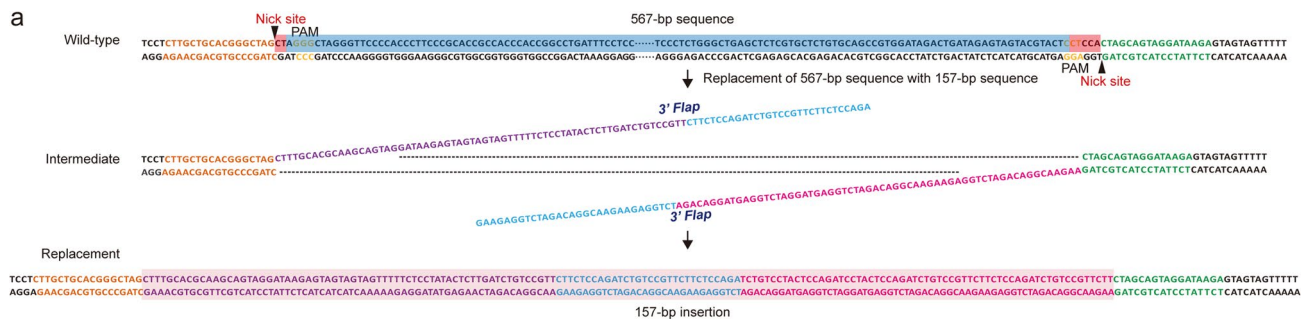
Fragment 13 Replacement of 4.8 kb with 34 bp (*lox76*): DualPE

Wild type	CGAAGATGAAACCAT	AGTCGGAACAGATAC	---	CTAAACCTCCCTCGCTTT	AGTCGTCGATAT	
Desired	CGAAGATGAAACCAT	ATAACTTCGTATAGCATACATTATACGCCGGT	ATTTAGTCGTCGATAT			
Accurate replacement	CGAAGATGAAACCAT	ATAACTTCGTATAGCATACATTATACGCCGGT	ATTTAGTCGTCGATAT			11759/113963
Imperfect replacement	CGAAGATGAAACCAT	ATAACTTCGTATAGCATACA	GTATACGCCGGT	ATTTAGTCGTCGATAT		112/113963

■ Desired replacement ■ SNP ■ Deletion

Extended Data Fig. 4 | Mutation type of byproducts for WT-DualPE and DualPE to generate replacement in wheat protoplasts. a, Schematic diagram of three types of outcomes for replacement. The resulted outcomes for replacement can be divided into three types. (1) accurate replacement, (2) imperfect replacement,

and (3) direct deletion. **b,c,** Represented byproducts which evaluated by high-throughput amplicon sequencing for 60-bp deletion with 38-bp insertion (b), and 4.8-kb deletion with 34-bp insertion (c).

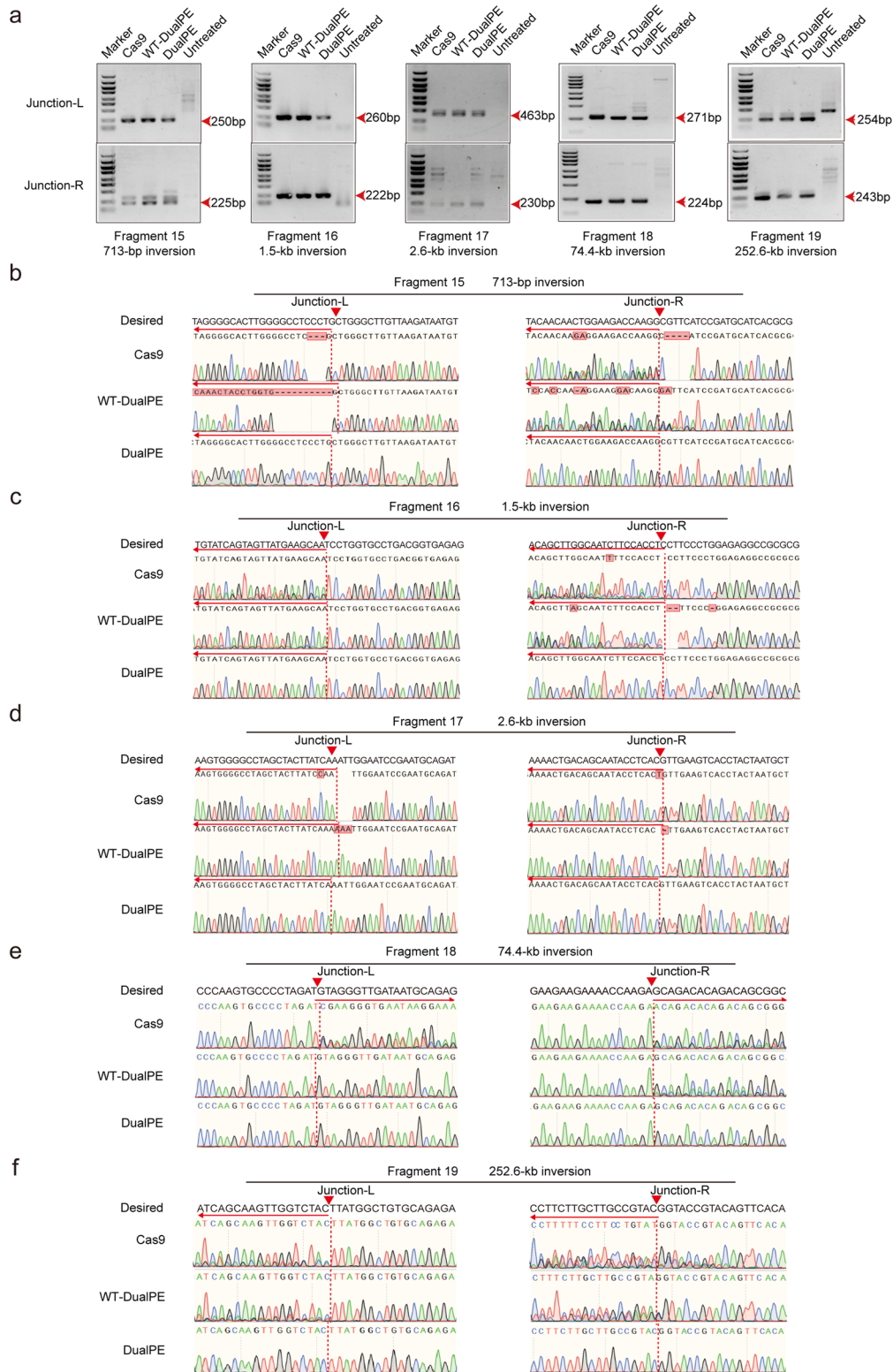


c

Plant ID	Genotype of T_0	No. of tested T_1 plants	Genotype of T_1		
			WT	HE	HO
T_0-2	HE	12	3	7	2
T_0-8	HE	34	8	18	8

Extended Data Fig. 5 | Identification and analysis of the replacement in wheat mutants at the site of *VRT-A2*. **a**, Schematic representation of the replacement of 567-bp sequence with 157 bp induced by DualPE. Spacers are shown in orange and green for *pegL* and *pegR*, respectively. RT templates encoding insertions marked as 3' flap are shown in purple and blue, and blue and pink for *pegL* and *pegR*, respectively. Homologous overlap between *pegL* and *pegR* is shown in

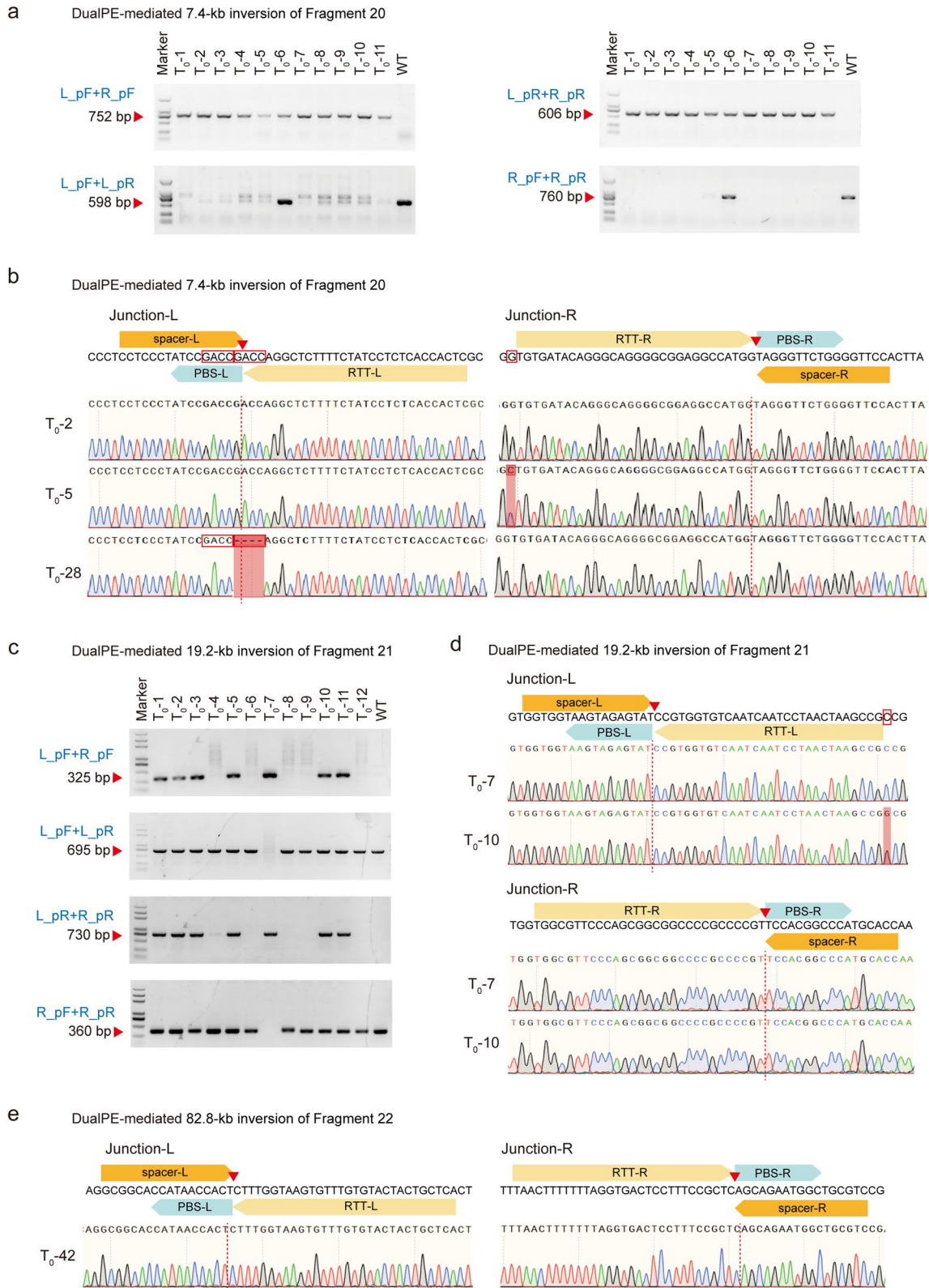
blue. The original 560 bp sequences are highlighted in blue, and the additional 7 bp flanking sequences that were deleted for PAM design are highlighted in red. The desired 157 bp insertion sequences are shown in purple, blue, and pink. **b**, Sanger sequencing chromatograms of T_0-2 , T_0-8 , T_0-12 , and T_0-14 . **c**, Segregation analysis of T_0-2 and T_0-8 lines derived from DualPE-mediated replacement. HO, homozygous; HE, heterozygous; WT, wild type.



Extended Data Fig. 6 | Gel electrophoresis of PCR products and Sanger sequencing chromatograms of inversion in wheat protoplasts.

a, Amplification of target genomic region using inversion-specific primers amplifying either junction-L or junction-R. The inversion amplicons are denoted with an red arrow. An untreated protoplasts sample served as control.

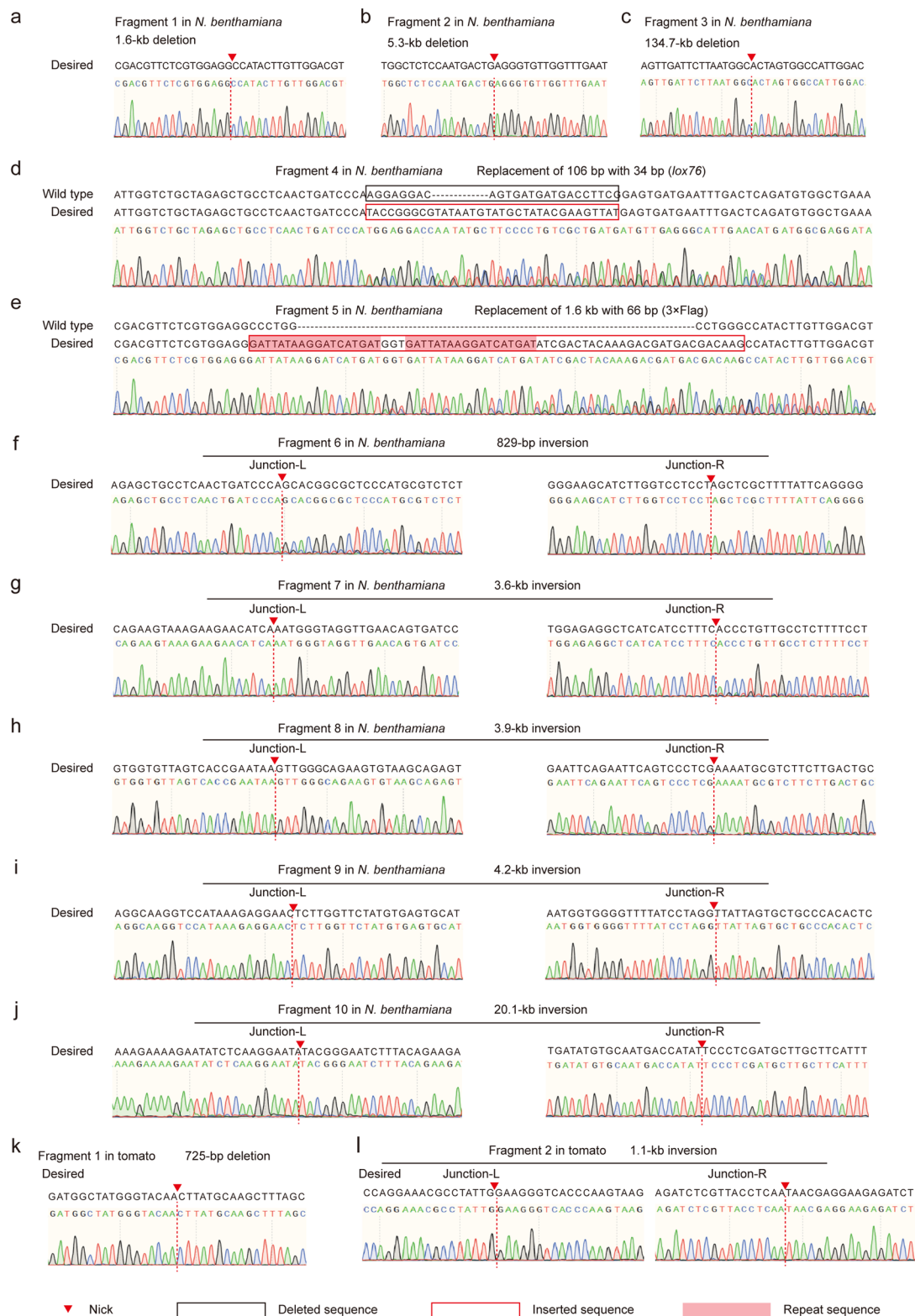
b-f, Sanger sequencing chromatograms of inversions induced by Cas9, WT-DualPE and DualPE at junction-L and -junction-R for sized 713-bp inversion (**b**), 1.5-kb inversion (**c**), 2.6-kb inversion (**d**), 74.4-kb inversion (**e**) and 252.6-kb inversion (**f**). Red arrows represent the junction of left or right.



Extended Data Fig. 7 | See next page for caption.

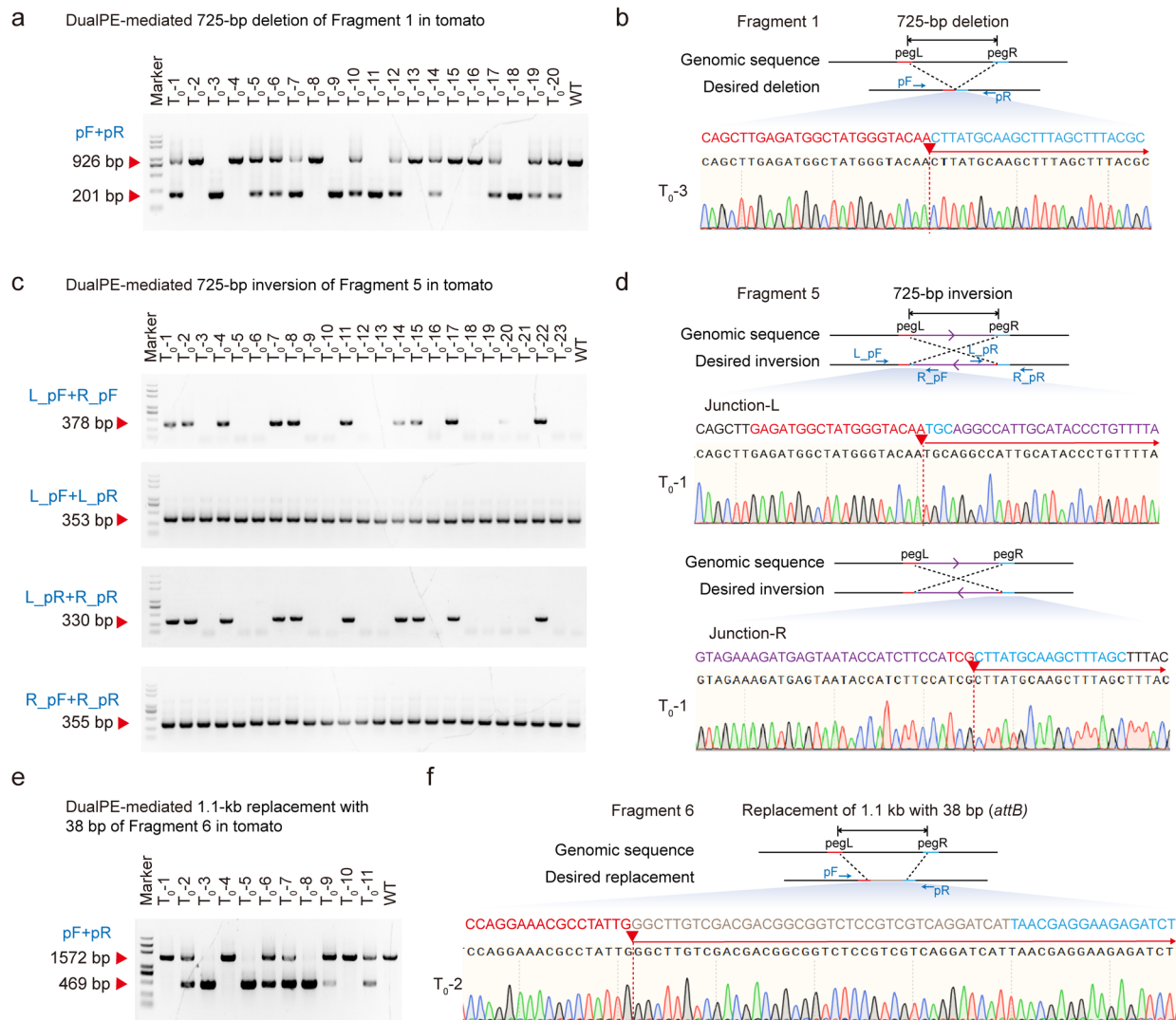
Extended Data Fig. 7 | Identification and analysis of the inversion for wheat mutants of Fragment 20-22. a, Representative agarose gel of PCR products for genotyping of the 7.4-kb inversion. The 752-bp band and the 606-bp band are the desired bands for the left and right junction of the inversion, respectively, while the 598-bp and the 760-bp bands are the expected size for the wild-type sequence. WT, wild-type. T₀-1, T₀-2, T₀-3, T₀-4, T₀-5, T₀-7, T₀-8, T₀-9, T₀-10, and T₀-11 were homozygous. **b**, Representative Sanger sequencing chromatograms of the 7.4-kb inversion mediated by DualPE in wheat plants. T₀-2 was identified as the precise inversion mutant at both Junction-L and Junction-R. In contrast, T₀-5 contained a single nucleotide polymorphism (SNP) at the intended Junction-R, likely resulting from byproducts associated with the pegRNA scaffold. Meanwhile, T₀-28 exhibited insertions and deletions (indels) at the targeted

Junction-L, which can be attributed to the presence of micro-homologous sequences. **c**, Representative agarose gel of PCR products for genotyping of the 19.2-kb inversion. The 325-bp band and the 730-bp band are the desired bands for the left and right junction of the inversion, respectively, while the 695-bp and the 360-bp bands are the expected size for the wild-type sequence. WT, wild-type. T₀-7 is homozygous. **d**, Representative Sanger sequencing chromatograms of the 19.2-kb inversion mediated by DualPE in wheat plants. T₀-7 was identified as the precise inversion mutant at both Junction-L and Junction-R. In contrast, T₀-10 contained a single nucleotide polymorphism (SNP) at the intended Junction-L, likely resulting from byproducts associated with the pegRNA scaffold. **e**, Representative Sanger sequencing chromatograms of the precise 82.8-kb inversion mediated by DualPE in wheat plants (T₀-42).



Extended Data Fig. 8 | Sanger sequencing chromatograms of large DNA editing induced by DualPE in *N. benthamiana* and tomato cells. a-c, Sanger sequencing chromatograms of precise deletions induced by DualPE in *N. benthamiana* for sized 1.6-kb deletion (a), 5.3-kb deletion (b), and 134.7-kb deletion (c). **d,e,** Sanger sequencing chromatograms of replacements induced by DualPE in *N. benthamiana* for replacement of 106 bp with 34 bp (d), and replacement of 1.6 kb with 66 bp (e). The repetitive sequence of the 3×Flag was

highlighted in red. **f-j,** Sanger sequencing chromatograms of precise inversions at junction-L and junction-R induced by DualPE in *N. benthamiana* for sized 829-bp inversion (f), 3.6-kb inversion (g), 3.9-kb inversion (h), 4.2-kb inversion (i), and 20.1-kb inversion (j). **k,l,** Sanger sequencing chromatograms of precise edits induced by DualPE in tomato for 725-bp deletion (k), 1.1-kb inversion (l). The red arrows represent the junction of two nick sites.



Extended Data Fig. 9 | Identification and analysis of DualPE-mediated large DNA mutants in tomato plants. **a**, Representative agarose gel of PCR products for genotyping of the 725-bp deletion. The 201-bp band is the desired size for the deletion, while the 926-bp band is the expected size for the wild-type sequence. T_0 -3, T_0 -9, T_0 -11 and T_0 -18 were homozygous. **b**, Sanger sequencing chromatograms of the precise 725-bp deletion. The left protospacer and right protospacer are shown in red and blue, respectively. **c**, Representative agarose gel of PCR products for genotyping of the 725-bp inversion. The 378-bp band and the 330-bp band are the desired bands for the left and right junction of the

inversion, respectively, while the 353-bp and the 355-bp bands are the expected size for the wild-type sequence. **d**, Sanger sequencing chromatograms of the precise 725-bp inversion. The left protospacer, right protospacer and inverted sequences are shown in red, blue and purple, respectively. **e**, Representative agarose gel of PCR products for genotyping of the 1.1-kb replacement with 38 bp. The 469-bp band is the desired size for the replacement, while the 1572-bp band is the size for the wild-type sequence. WT, wild-type control plant. T_0 -3, T_0 -5 and T_0 -8 were homozygous. **f**, Sanger sequencing chromatograms of the precise 1.1-kb replacement with 38 bp. The desired replacements are shown in brown.

a

b

Design	Target sequence (5'-3')-PAM	PBS	RTT	Distance [?]	Forward primer (5'-3')	Reverse primer (5'-3')	Sequence after deletion	
No. 1 recommended program Desired Deletion!	pegL	TCTGCCATCTCTGGTTTT GGG	ACCAGGAGAT Length: 10 Tm: 30°C	TCCTGAGCCGGGG GCCTCTCCAGGAA GG Length: 30	0	TGTTCACTGCCGTATAGT TGCCCATCTCTGGTTTTGT TTAAGAGCTATGCTGG	GTAAGTATAGAACCGCG ACCAGGAGATCTCTGAGCC GCGGGCCTCTCCAGGGA AGGGCACCAGCTCGGTGC CA	AATCTTCAGCGTTGGGTCAAT CTGGTATATTTCTGCCATCTC CTGGTCTCTCCCTGAGAGGC GCGCGGCTCAGGACGGCGC CTGCAATGCAAGGA
	pegR	GGCCTCTCCAGGGAAGTCC TGG	CCTTCCCTG Length: 9 Tm: 30°C	ATCTGTATATTTCT GCCCATCTCTGGT Length: 30	0	TGTTCACTGCCGTATAGG GCCTCTCCAGGGAAGTCC GTTAAGAGCTATGCTGG	GTAAGTATAGAACCGCG CCTTCCCTGATCTGTATAT TTTCTGCCATCTCTGGTG CACCAGCTCGGTGCCA	
No. 2 recommended program Others (This result is within the user-specified ranges)	pegL	TTCTGCCATCTCTGGTTTT TGG	CCAGGAGATG Length: 10 Tm: 32°C	TCCTGAGCCGGGG GCCTCTCCAGGAA GG Length: 30	1	TGTTCACTGCCGTATAGT CTGCCATCTCTGGTTTTGT TTAAGAGCTATGCTGG	GTAAGTATAGAACCGCG CCAGGAGATGCTCTGAGCC GCGGGCCTCTCCAGGGA AGGGCACCAGCTCGGTGC CA	AATCTTCAGCGTTGGGTCAAT CTGGTATATTTCTGCCATCTC CTGGCCTCTCCCTGAGAGGC GCGCGGCTCAGGACGGCGC TGCAATGCAAGGA
	pegR	GGCCTCTCCAGGGAAGTCC TGG	CCTTCCCTG Length: 9 Tm: 30°C	AATCTGTATATTT CTGCCATCTCTGG G Length: 30	0	TGTTCACTGCCGTATAGG GCCTCTCCAGGGAAGTCC GTTAAGAGCTATGCTGG	GTAAGTATAGAACCGCG CCTTCCCTGATCTGTATA TTTCTGCCATCTCTGGTG CACCAGCTCGGTGCCA	

Extended Data Fig. 10 | Input and output page of the dual-pegRNA designing webserver. a, The input page of DualPE-Finder webserver includes the input textbox, user-defined parameters and primer design. **b**, Output page of DualPE-Finder webserver. The webserver displays all possible candidate pegLs and

pegRs, providing details on spacer, PBS, RTT, primers and sequence after editing. Candidates are recommended based on the cumulative distance of pegL nicking from the start position and pegR nicking from the end position of the desired editing fragments, specifically ranked from the shortest to the longest distance.

Reporting Summary

Nature Portfolio wishes to improve the reproducibility of the work that we publish. This form provides structure for consistency and transparency in reporting. For further information on Nature Portfolio policies, see our [Editorial Policies](#) and the [Editorial Policy Checklist](#).

Statistics

For all statistical analyses, confirm that the following items are present in the figure legend, table legend, main text, or Methods section.

- | n/a | Confirmed |
|-------------------------------------|--|
| <input type="checkbox"/> | <input checked="" type="checkbox"/> The exact sample size (n) for each experimental group/condition, given as a discrete number and unit of measurement |
| <input type="checkbox"/> | <input checked="" type="checkbox"/> A statement on whether measurements were taken from distinct samples or whether the same sample was measured repeatedly |
| <input type="checkbox"/> | <input checked="" type="checkbox"/> The statistical test(s) used AND whether they are one- or two-sided
<i>Only common tests should be described solely by name; describe more complex techniques in the Methods section.</i> |
| <input checked="" type="checkbox"/> | <input type="checkbox"/> A description of all covariates tested |
| <input checked="" type="checkbox"/> | <input type="checkbox"/> A description of any assumptions or corrections, such as tests of normality and adjustment for multiple comparisons |
| <input type="checkbox"/> | <input checked="" type="checkbox"/> A full description of the statistical parameters including central tendency (e.g. means) or other basic estimates (e.g. regression coefficient) AND variation (e.g. standard deviation) or associated estimates of uncertainty (e.g. confidence intervals) |
| <input type="checkbox"/> | <input checked="" type="checkbox"/> For null hypothesis testing, the test statistic (e.g. F , t , r) with confidence intervals, effect sizes, degrees of freedom and P value noted
<i>Give P values as exact values whenever suitable.</i> |
| <input checked="" type="checkbox"/> | <input type="checkbox"/> For Bayesian analysis, information on the choice of priors and Markov chain Monte Carlo settings |
| <input checked="" type="checkbox"/> | <input type="checkbox"/> For hierarchical and complex designs, identification of the appropriate level for tests and full reporting of outcomes |
| <input checked="" type="checkbox"/> | <input type="checkbox"/> Estimates of effect sizes (e.g. Cohen's d , Pearson's r), indicating how they were calculated |

Our web collection on [statistics for biologists](#) contains articles on many of the points above.

Software and code

Policy information about [availability of computer code](#)

Data collection Illumina NovaSeq platform was used to collect the high-throughput amplicon sequencing data.

Data analysis Amplicon sequencing data of prime-editing processivity was analyzed using the published code in reference 55. Graphpad prism 8.0.1 was used to analyze the data. QIAcuity Software Suite (version 2.5.0.1) was used to analyze the results of digital PCR. We have deposited the code of webserver for dual-pegRNA design used at Github (<https://github.com/ZongyuanLab/DualPE>).

For manuscripts utilizing custom algorithms or software that are central to the research but not yet described in published literature, software must be made available to editors and reviewers. We strongly encourage code deposition in a community repository (e.g. GitHub). See the Nature Portfolio [guidelines for submitting code & software](#) for further information.

Data

Policy information about [availability of data](#)

All manuscripts must include a [data availability statement](#). This statement should provide the following information, where applicable:

- Accession codes, unique identifiers, or web links for publicly available datasets
- A description of any restrictions on data availability
- For clinical datasets or third party data, please ensure that the statement adheres to our [policy](#)

Raw sequencing data has been deposited in the National Center for Biotechnology Information Sequence Read Archive database with the BioProject accession code PRJNA1192508. Datasets of high-throughput sequencing experiments can be publicly released before publication.

Research involving human participants, their data, or biological material

Policy information about studies with [human participants or human data](#). See also policy information about [sex, gender \(identity/presentation\), and sexual orientation](#) and [race, ethnicity and racism](#).

Reporting on sex and gender	N/A
Reporting on race, ethnicity, or other socially relevant groupings	N/A
Population characteristics	N/A
Recruitment	N/A
Ethics oversight	N/A

Note that full information on the approval of the study protocol must also be provided in the manuscript.

Field-specific reporting

Please select the one below that is the best fit for your research. If you are not sure, read the appropriate sections before making your selection.

Life sciences Behavioural & social sciences Ecological, evolutionary & environmental sciences

For a reference copy of the document with all sections, see nature.com/documents/nr-reporting-summary-flat.pdf

Life sciences study design

All studies must disclose on these points even when the disclosure is negative.

Sample size	The experiments of protoplasts were performed with three biological repeats. About 500,000 protoplasts were used for each transfection. The number of protoplasts in each transfection was measured by thrombocytometry. The experiment in wheat and tomato regenerated plants were performed once. All the regenerated seedlings were sampled, the number of mutants were confirmed by Sanger sequencing.
Data exclusions	No data exclusion.
Replication	All attempts for replication were successful. For the experiments in wheat protoplasts, tomato protoplasts, genotyping of transgenic plants and <i>Nicotiana benthamiana</i> infiltration, a minimum of three independent experiments were included.
Randomization	Wheat and tomato protoplasts were isolated and randomly separated to each transformation.
Blinding	Not applicable. As samples were processed identically through standard and in some cases automated procedures (DNA sequencing, transfection, DNA isolation) that should not bias outcomes.

Reporting for specific materials, systems and methods

We require information from authors about some types of materials, experimental systems and methods used in many studies. Here, indicate whether each material, system or method listed is relevant to your study. If you are not sure if a list item applies to your research, read the appropriate section before selecting a response.

Materials & experimental systems

n/a	Involved in the study
<input checked="" type="checkbox"/>	<input type="checkbox"/> Antibodies
<input checked="" type="checkbox"/>	<input type="checkbox"/> Eukaryotic cell lines
<input checked="" type="checkbox"/>	<input type="checkbox"/> Palaeontology and archaeology
<input checked="" type="checkbox"/>	<input type="checkbox"/> Animals and other organisms
<input checked="" type="checkbox"/>	<input type="checkbox"/> Clinical data
<input checked="" type="checkbox"/>	<input type="checkbox"/> Dual use research of concern
<input type="checkbox"/>	<input checked="" type="checkbox"/> Plants

Methods

n/a	Involved in the study
<input checked="" type="checkbox"/>	<input type="checkbox"/> ChIP-seq
<input checked="" type="checkbox"/>	<input type="checkbox"/> Flow cytometry
<input checked="" type="checkbox"/>	<input type="checkbox"/> MRI-based neuroimaging

Dual use research of concern

Policy information about [dual use research of concern](#)

Hazards

Could the accidental, deliberate or reckless misuse of agents or technologies generated in the work, or the application of information presented in the manuscript, pose a threat to:

- | No | Yes | |
|-------------------------------------|--------------------------|----------------------------|
| <input checked="" type="checkbox"/> | <input type="checkbox"/> | Public health |
| <input checked="" type="checkbox"/> | <input type="checkbox"/> | National security |
| <input checked="" type="checkbox"/> | <input type="checkbox"/> | Crops and/or livestock |
| <input checked="" type="checkbox"/> | <input type="checkbox"/> | Ecosystems |
| <input checked="" type="checkbox"/> | <input type="checkbox"/> | Any other significant area |

Experiments of concern

Does the work involve any of these experiments of concern:

- | No | Yes | |
|-------------------------------------|--------------------------|---|
| <input checked="" type="checkbox"/> | <input type="checkbox"/> | Demonstrate how to render a vaccine ineffective |
| <input checked="" type="checkbox"/> | <input type="checkbox"/> | Confer resistance to therapeutically useful antibiotics or antiviral agents |
| <input checked="" type="checkbox"/> | <input type="checkbox"/> | Enhance the virulence of a pathogen or render a nonpathogen virulent |
| <input checked="" type="checkbox"/> | <input type="checkbox"/> | Increase transmissibility of a pathogen |
| <input checked="" type="checkbox"/> | <input type="checkbox"/> | Alter the host range of a pathogen |
| <input checked="" type="checkbox"/> | <input type="checkbox"/> | Enable evasion of diagnostic/detection modalities |
| <input checked="" type="checkbox"/> | <input type="checkbox"/> | Enable the weaponization of a biological agent or toxin |
| <input checked="" type="checkbox"/> | <input type="checkbox"/> | Any other potentially harmful combination of experiments and agents |

Plants

Seed stocks

We used the Immature embryo the bread wheat cultivar Fielder and the cotyledons from *S. lycopersicum* (L.) cv. Alisa Craig (AC) for genetic transformation. For the wheat and tomato mutants used for trait evaluation, the growing conditions and collection method are detailed in the methods.

Novel plant genotypes

Binary plasmid pB-DualPE or pH-EF1 α -DualPE containing the dual-epegRNA array was transformed into the bread wheat cultivar Fielder or *S. lycopersicum* (L.) cv. Alisa Craig (AC) using Agrobacterium-mediated gene transformation. The endogenous sequence targeted for editing and the targeting guide RNA sequence is shown in Supplementary table 1.

Authentication

Different genotypes can be distinguished through PCR primers in the Supplementary table 4.